

## Article

# Characteristics of Land-Use Carbon Emissions and Carbon Balance Zoning in the Economic Belt on the Northern Slope of Tianshan

Gulmira Abbas<sup>1</sup> and Alimujiang Kasimu<sup>1,2,\*</sup> <sup>1</sup> School of Geography and Tourism, Xinjiang Normal University, Urumqi 830054, China; gulmira091@126.com<sup>2</sup> Urbanization Development Research Center of the Silk Road Economic Belt, Xinjiang Normal University, Urumqi 830054, China

\* Correspondence: alimkasim@xjnu.edu.cn; Tel.: +86-150-9907-9312

**Abstract:** How to identify variables for carbon reductions was considered as one of the most important research topics in related academic fields. In this study, the characteristics of landuse carbon emissions of the economic belt on the northern slope of Tianshan (NST) were tentatively investigated. Taking 12 cities in NST as the case study, land use carbon emissions and carbon intensities were estimated and analyzed based on the Landsat remote sensing image and socio-economic statistical data in 1990, 2000, 2010, and 2020. Moreover, Moran's I model was applied to study spatial autocorrelation between carbon emissions and carbon intensities. Results show that (1) urban land and cropland were increased rapidly during the past three decades; (2) carbon emissions were increasing significantly, and the urban land was responsible for the majority of the carbon emission; (3) negative spatial correlations on both net carbon emissions and carbon intensities were obtained between 12 cities; and (4) based on carbon balance zoning analysis, NST could be divided into four different zones. The rising ratio of carbon emissions and intensities was significantly higher than urbanization expending speed. Results could provide references and useful insights into related arrangements of policies and attempts on carbon reduction for cities in NST.

**Keywords:** land-use change; carbon emissions; spatial autocorrelation; carbon balance zoning; the economic belt in northern slope of Tianshan



**Citation:** Abbas, G.; Kasimu, A. Characteristics of Land-Use Carbon Emissions and Carbon Balance Zoning in the Economic Belt on the Northern Slope of Tianshan. *Sustainability* **2023**, *15*, 11778. <https://doi.org/10.3390/su151511778>

Academic Editor: Wen-Hsien Tsai

Received: 8 June 2023

Revised: 22 July 2023

Accepted: 23 July 2023

Published: 31 July 2023



**Copyright:** © 2023 by the authors. Licensee MDPI, Basel, Switzerland. This article is an open access article distributed under the terms and conditions of the Creative Commons Attribution (CC BY) license (<https://creativecommons.org/licenses/by/4.0/>).

## 1. Introduction

Promoting low-carbon development and carbon emission control became one of the most common consensuses for the international community and related organizations due to the serious increases in global warming and the environmental crisis [1]. Carbon emissions (CEs) were proven to be the most contributing factor for global climate change, and arousal of CO<sub>2</sub> content in the airspace is considered as the main cause for global warming and the greenhouse effect [2,3]. Studies indicate that fossil fuels combustion, land use, and other human activities, which led to a series of problems associated with resources and the environment, were considered to be the main causes for carbon emissions (Figure 1) [4]. According to the global statistics, the CE amounts of China took on the highest value since 2006, and it was reported that rapid urbanization is the greatest contributor to CE growth [5]. Therefore, to develop a low-carbon area by sustainable planning, it is imperative to comprehensively understand the characteristics and spatial patterns of carbon transitions, the sources and influencing factors of CEs, and especially, to investigate how land-use changes effect carbon balance (carbon emissions and carbon absorptions).

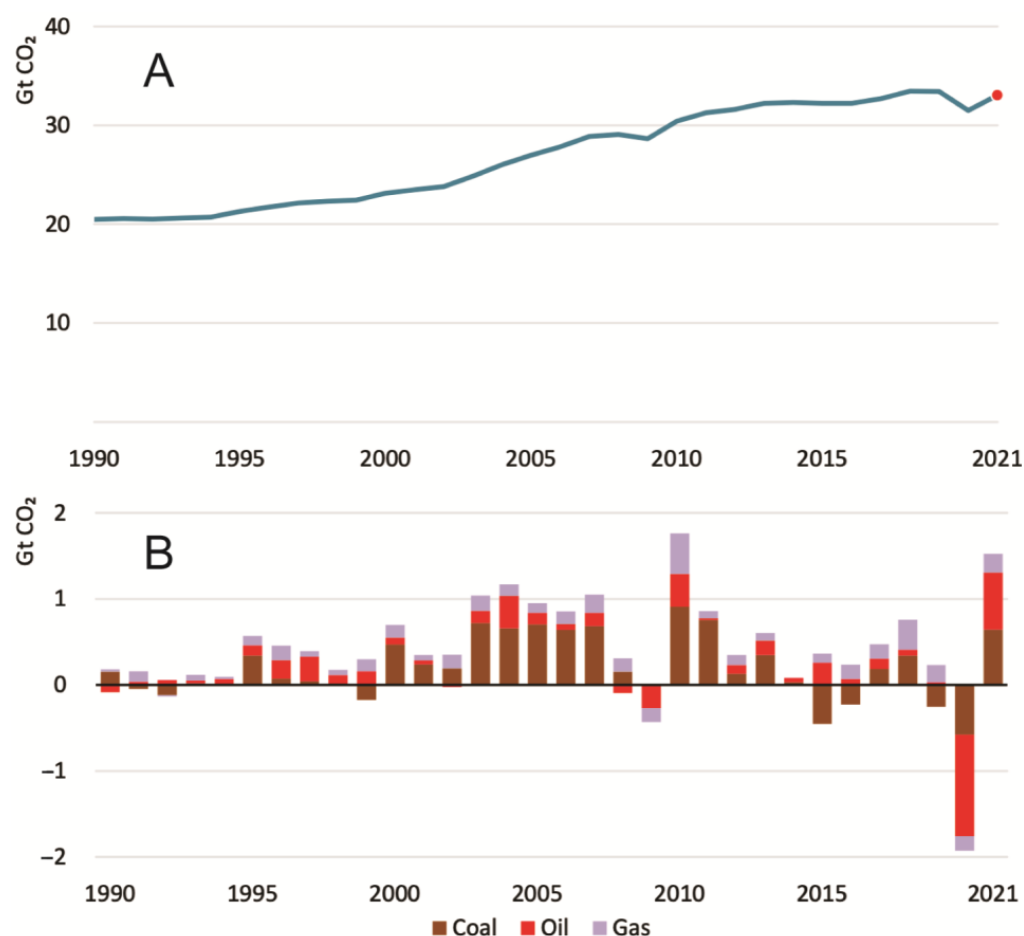


**Figure 1.** Global energy-related CO<sub>2</sub> emissions (A), and change in CO<sub>2</sub> emissions (B) by fuel, 1990–2021. Source: IEA 2021.

Studies on effecting factors of carbon balance were one of the hot topics in the research fields. Investigations on the existing data and projects, such as the Global Carbon Project (GCP) and World Resources Institute (WRI), illustrated the five main inventoried carbon emission fields, including energy consumptions, industry, agriculture, and land-use changes, respectively [6–9]. Among them, the fossil fuels and land use, land-use change, and forestry (LULUCF) were considered as the main sources of CEs [10]. Previous articles also revealed that the main sources of CEs from land use were mainly the activities of mankind on the land, as well as the maintenance of and changes in the land itself [11]. Meanwhile, land is a field and vital effecting factor for CEs from energy consumption. Thus, it was suggested that human activities on the land were the greatest factor for [12]. Most of the human activities were carried by land, and the land-use structures of different countries and areas are different to some extent, and accordingly, the mechanism of land-use CE was complex and contains several uncertain factors [13]. Comprehensive studies on land-use CE and its characteristics were beneficial for improving the calculation accuracy of CEs, by which the affecting factors would be further clarified [14–16]. In addition, the concrete analysis on specific issues could be implemented via focalized studies on sectional land-use CEs, which is greatly conducive with the adjustment of land-use structure and further formulation of relevant policies on CE reduction [17].

Investigations on land-use carbon emissions are mainly focused on land-use changing characteristics and influencing factors, and mostly considered from various aspects, including land intensive, carbon emission effect, energy consumptions, and land-use optimization [18]. Several studies focused on the topics related to land-use carbon emission inventories, improving policy proposing, and greenhouse gas reductions in Asian regions [19,20]. In China, nevertheless, related studies were relatively rare, and mostly conducted on a province level. Zhang Laihuang et al., taking the different regions in China as the case study, conducted the carbon intensity (CI) analysis derived by the transformation between land-use types, and found great differences in carbon intensity between different domains [21]. Cui Yifang et al., using the Landsat image data of the Yangtze River Delta urban agglomeration, performed land-use carbon emissions analysis and estimations for the 1994–2016 time period. A total of 26 cities was selected and the CEs and CIs were estimated by using the carbon emission coefficients referenced from published data, and the autocorrelation between CEs and CIs was analyzed with the help of spatial autocorrelation models. Results indicate that CIs of cities in Anhui province had relatively lower CIs compared to other cities in the studied area [22]. Xia Chuyu et al. analyzed urban carbon metabolism and mapped the spatial processes by applying the land-use and cover change from 1995 to 2015 of 13 cities in the Yangtze River Delta. Furthermore, the connection between urban size growth and urban carbon metabolism was preliminarily studied based on the panel data regression analysis [23]. Results illustrate that carbon transition mainly contributed to the changes in industrial or transportation land. Previous research provided robust methodology for land-use carbon transitions and metabolisms, and provided insights into the development of low-carbon cities by controlling or managing the land-use changes [23]. However, in Xinjiang, such studies are very limited, specifically in the northern slope of Tianshan Mountain (NST), comprehensive studies, which integrated energy consumption, land-use change, and carbon emission in the particular context of cities or areas, are not available.

Several statistical methods and analytical approaches were widely applied for the related studies on land-use carbon emissions (Table 1) [24,25]. Recently, remote sensing (RS) technology was proven to be a powerful tool for CEs estimation due to its transparency, multi-time qualities, and wide coverage [26,27]. However, to create an inventory of CO<sub>2</sub> and carbon stock changes over time, the combination of more software with remote sensing technology is necessary [28,29].

Using the data calculation on CEs of different land-use types, a research team found increasing trends in total land-use carbon emissions and per capita carbon emissions in Xinjiang, and the correlation degree between land-use structure and CEs was found to be different based on the gray correlation analysis [30]. Some researchers investigated the relationship of land-use changes, CEs, and energy consumption for a metropolis in Pakistan [31]. Numerous findings suggested that it is possible to control CEs from energy consumption with the help of adjusting the land-use structure [32–35]. Taking Kunming City, Yunnan Province, China, as the research area, Li Zhang and Ping Wang studied the changing characteristics of land uses, and further investigated the correlation of land-use structure and CEs from energy consumption. Results show a close correlation [36]. A study on CEs in the field of LULUCF in the Vietnam mainland applied 10 years of land cover change data (2002–2012) as sources, processed those data with a specific software (ALU, v2014), and estimated the CEs based on the quality control and quality assurance work [37]. Some typical related research on CEs, land-use changing characteristics, and NST are listed in Table 1 [32–35,38–43]. A large number of previous works demonstrated the promising future and high efficiency of methods for land-use CEs calculation and relative correlation analysis based on the remote sensing (RS) data classification and the statistical data analysis via software processing.

**Table 1.** Literature summary.

Author	Countries	Period	Methods/Model	Results
[32]	China	2005–2017	Environmentally extended input–output model	Higher CEs; overall efficiency of CE improved; the reduction potential: embodied CEs < direct CEs.
[33]	Sichuan, China	2000–2018	Corrected carbon emission coefficient method	Higher CEs; CEs were correlated with GDP.
[34]	India	2006–2021	Threshold regression model	Foreign trade investment greatly affected the industrial CEs both positively and negatively.
[35]	China	2000–2017	Dynamic panel models Green Solow model	Total technological progress is helpful to reducing carbon emissions; production technology remarkably drives carbon emissions.
[38]	Tibetan plateau, China	2012–2017	Net primary productivity (NPP) remote estimation model Structural decomposition analysis model	Great potential for carbon neutrality was observed for Tibet; energy consumption was the major contributor for CEs growth.
[39]	China	2003–2019	Time-varying DID model Mediating model	National Industrial Relocation Demonstration Zones effectively reduced CEs, and its impacts are various.
[40]	China	2000–2019	Carbon emission model The decoupling analysis	Construction land is the primary and important contributor to CEs; the decoupling between land use and CEs is dynamic. CEs from land use are heterogeneous.
[41]	Global	2000–2019	Super-EBM model Tobit model	A great difference in CE efficiency among 136 different countries; the CEs efficiency of most countries are not ideal; the CE efficiency supports the EKC hypothesis; urbanization level; economy and energy improved the CEs efficiency.
[42]	China	2000–2020	Modified gravity model Social network analysis method	The comprehensive development quality level of cities on NST increased; the economic linkages existed in an obvious central orientation and geographical proximity.
[43]	China	2000–2020	Principal component analysis Unary linear regression Spatial autocorrelation analysis	The environmental quality was graded as poor for more than 40% of the region; the overall trend was toward increasing the areas with good and excellent grades; a spatial relationship between environmental quality and human disturbances is positive.

In terms of research scale, large-scale studies were conducted for the overall analysis of regions or countries, and for the global level [44]. Meanwhile, medium- and small-scale research was conducted for better understanding and explicit interpretation of land-use CEs and other related topics [45]. With the construction and development of the Silk Road economic belt, NST was considered as an economic core area in China, and its ecological and environmental issue received significant attention in academic fields. The urban agglomeration of NST is the area with the highest level of urbanization, the densest population with abundant gross domestic product (GDP), and the most concentrated industries in Xinjiang [46]. Moreover, in the future, this area will become a strategic core region of economic development. In addition, various country level strategies and global terms suggested the importance of considerations on environmental protection for NST during the sustainable development process. As such, promoting the eco-friendly development of the region is of great significance [47]. As a region that is undergoing rapid speed on urbanization, economic development, and industrialization, an urban agglomeration (UA) plays a core function in regional and even affect national CEs. Accordingly, UA is also a key contributor for the reduction in regional CEs. For sustainable development and high-quality growth of UAs in China, it is imperative to conduct researches on CEs [46]. Several studies focused on CE investigations in various typical areas in the country [35,41];

however, studies on CEs from newly developing UAs are rare. Comprehensive analysis on characteristics of land-use CEs for this area is of significance and remains to be conducted.

To better understand the current states and characteristics of CEs and land-use changing dynamics, in this study, land-use changing characteristics and the current status of carbon balance, including carbon emissions, carbon absorptions, and carbon intensity, in the NST were preliminarily investigated (Figure 2). Furthermore, CE reduction improving suggestions on policies was tentatively proposed. The findings of this study could provide a scientific base for comprehensive understanding of the future urbanization of NST, and could also be considered as a reference for different land-use stakeholders.

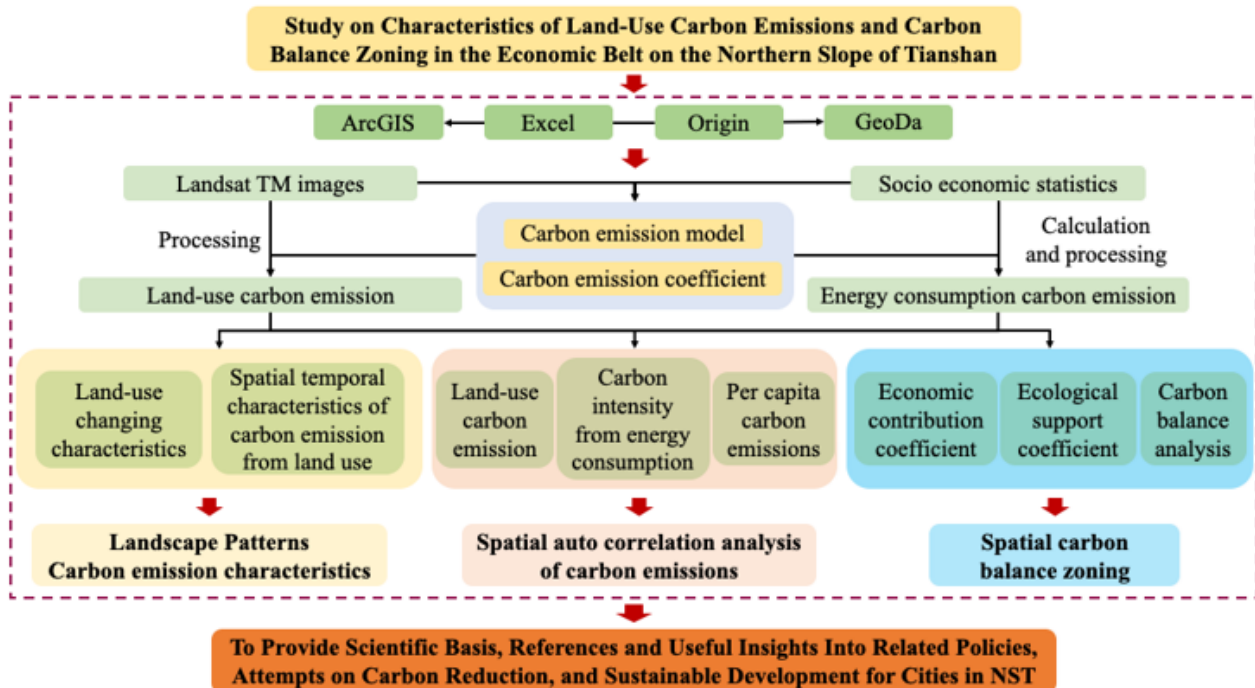


Figure 2. The research framework and path diagram.

## 2. Materials and Methods

### 2.1. Study Area

The study section is located on the northern slope of the Tianshan Mountain, which is in the hinterland of the Eurasian continent. This is a long and narrow area at 42°50′–46°12′ N north latitude and 79°53′–92°06′ E east longitude (Figure 3). The spatial scope includes 12 cities as shown in Figure 2. This area is about  $14.66 \times 10^4$  km<sup>2</sup> in size, accounting for 8.78% of Xinjiang, with a population of over 4.5 million, which is accounting for over 23% of this province [48,49]. The southern area is a mountainous region (800–4000 m above sea level), the middle part is mainly covered by oases (450–500 m above sea level), while the northern part is typical desert land (440–460 m above sea level). The ecosystem and environment of this area is extraordinarily fragile, wherein the majority of Greenland was damaged and vanished, and eventually replaced and substituted by an artificial oasis [50].

The term of “the northern slope of the Tianshan Mountain” is proposed firstly in “China’s western development strategy—the development strategy of Xinjiang” program, and became an economic hot zone in 2001 [51]. Continually, this area was confirmed as one of the 18 key areas of China in the same year, and stands as a core area for the economic development of Xinjiang province. More importantly, this place is also considered as a strong supporting region for “the China’s western development” strategy, and “the belt and road” strategy [52]. The importance of strategies and economic development induced vigorous development of land use and other sides, which could cause certain changes in carbon balances and ecosystems [53]. More data references and analytical results about the characteristics of land-use CEs could be expected from this study.

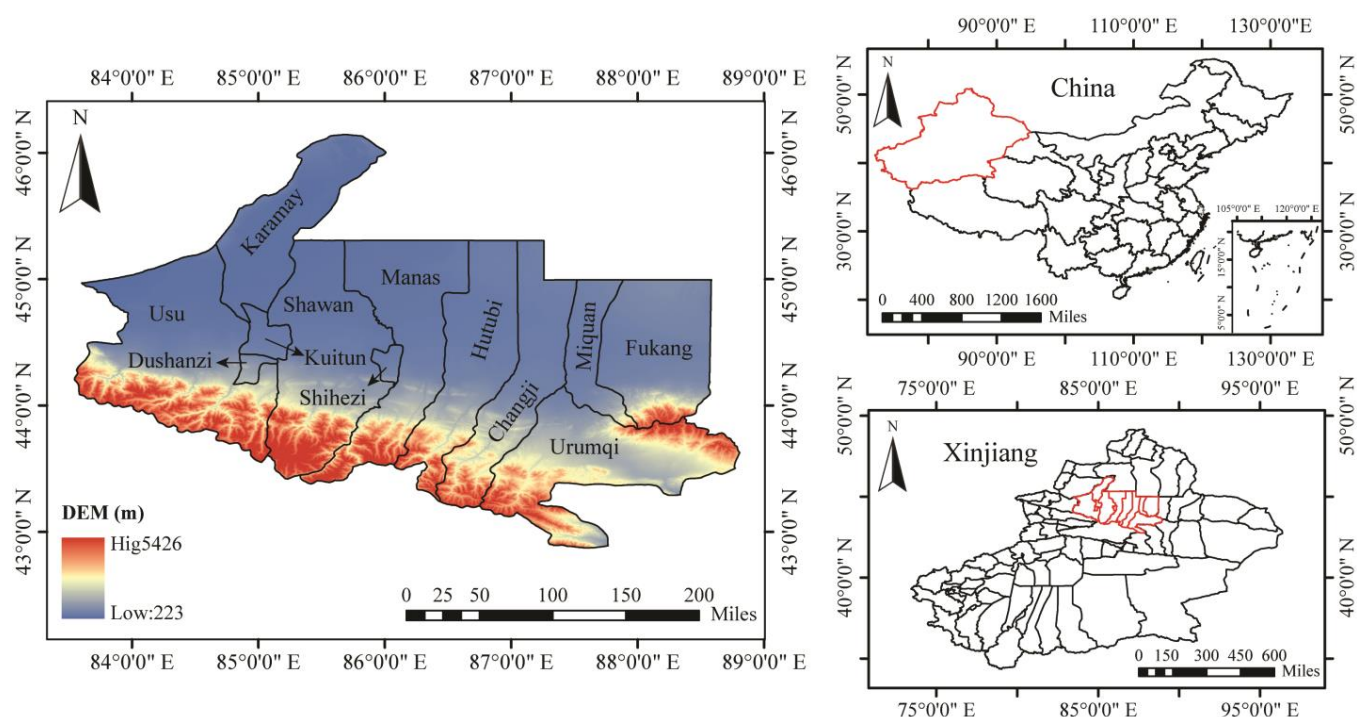


**Figure 3.** The map of study region.

## 2.2. Data

There are two different types of data, including the remote sensing data and the socio-economic statistical data, for land-use changing characteristics analysis and land-use carbon metabolism analysis, respectively.

The land-use data were interpreted and derived from remote sensing images (from Chinese Academy of Sciences Environment and Resources Center, [www.resdc.cn](http://www.resdc.cn) (accessed on 20 January 2021), 1.0 km), which provide detailed, spatiotemporal, and accurate land mapping information. The remote sensing images of land-use changes for different time periods were acquired from the Chinese Academy of Science Environment and Resources Center ([www.resdc.cn](http://www.resdc.cn) (accessed on 20 January 2021), 1.0 km). Subsequently, the cloud-free Landsat TM image data of 1990, 2000, 2010, and 2020 were selected for further study. These data identified 25 types of land use, and the carbon metabolism concept model was built based on those types. A classification of six land utilization patterns, including cropland, forestland, grassland, water area, urban land, and other land uses, were established based on the landscape features of the objective area. In addition, empirical coefficients were applied to calculate CEs and carbon sequestration; then, special analyst tools in ArcGIS10.2 were utilized to investigate the special models of CEs. Furthermore, panel data analysis was carried out to discuss the characteristics of land-use CEs at the final stage. These types presented as referred artificial and natural factors for CEs calculation. The data were preprocessed and taken for overlay analysis and spatial statistical analysis for image interpretation, and finally, output as an image (Figure 4).

## 2.3. Socio-Economic Statistics

For carbon metabolism (carbon emissions and carbon intensity) analysis, energy consumption data and GDP data were considered as two important inputs [54,55]. The above data of 12 places were acquired from city-level statistical yearbooks or provincial statistical yearbooks (data were shown in Table S1). Generally, quantities for major types of energy consumption were offered annually in corresponding statistical reports, and commonly available. Nevertheless, the statistical data collection procedure showed that some particular data types were not detailed in the specific yearbooks. These energy-related necessary data were acquired from the local statistics departments.

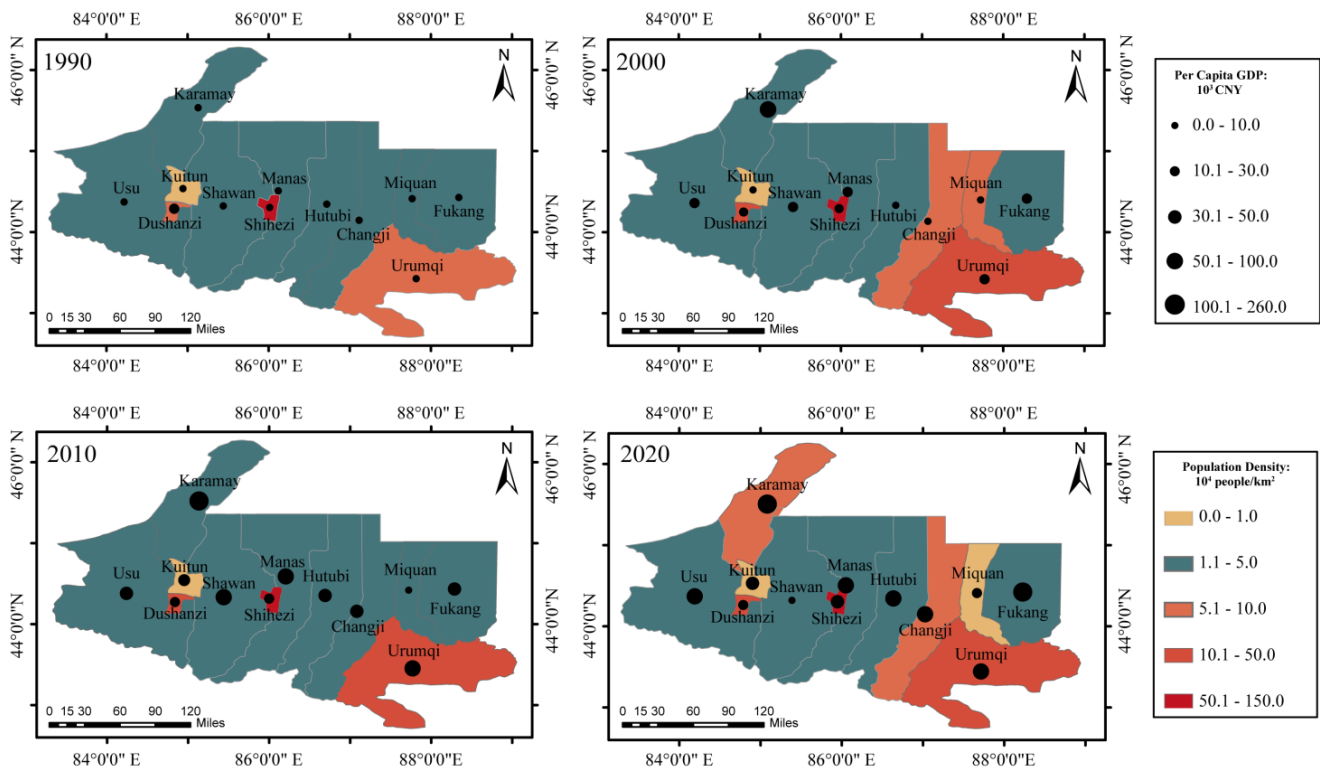


**Figure 4.** The general characteristics of 12 places in the economic belt on the northern slope of Tianshan.

## 2.4. Methodology

### 2.4.1. Land-Use Structure Evaluation

The evaluating methodology of land-use CE estimation under the background of landscape patterns was established (Figure 5). These categories were named as cropland, forestland, urban land, grassland, water areas, and other land uses, separately [56,57].

### 2.4.2. Carbon Emissions from Land Use

Land-use CEs corresponding to the released CO<sub>2</sub> originated from land-use changes and human activities [58]. During the land using process, a series of changes were produced to the terrestrial ecosystem, which caused the transformation and variation in carbon storage. Land uses were divided into land-use conversion type and unchanged land-use type according to the 2006 Intergovernmental Panel on Climate Change (IPCC) Guidelines. Consequently, CEs from land use could also be classified into direct CEs and indirect CEs, respectively. Direct CEs were generated by land-use type transformation, while the indirect CEs were mainly produced by human activities on different land-use types [59]. The focus of this study was the CEs produced from the land-use changes.

Previous research results illustrate the methods for calculation of CEs [32,33], and the following equation (Equation (1)) was applied for the calculation in this work:

$$E_i = \sum e_i = \sum s_i \times \delta_i \times \frac{M_{CO_2}}{M_C}, \quad (1)$$

of which  $E_i$  is CE from land use;  $i$  refers to land-use types;  $S_i$  is the region area of land  $i$ ; and  $\delta_i$  is the carbon emission coefficient (CEC) for land  $i$ . Positive values of CECs indicate CE, while minus values indicate carbon absorption (CA);  $M_{CO_2}/M_C$  represented the ratio of relative molecular weight of CO<sub>2</sub> to carbon: 44/12. In previous studies, different CECs were calculated for different land-use types and applied for related calculations [50,51]. Those values were referred to in this study directly or meaningfully in our investigation (Table 2). It was obvious that the CECs of forestland and grassland were comparatively small, yet the difference was remarkable.

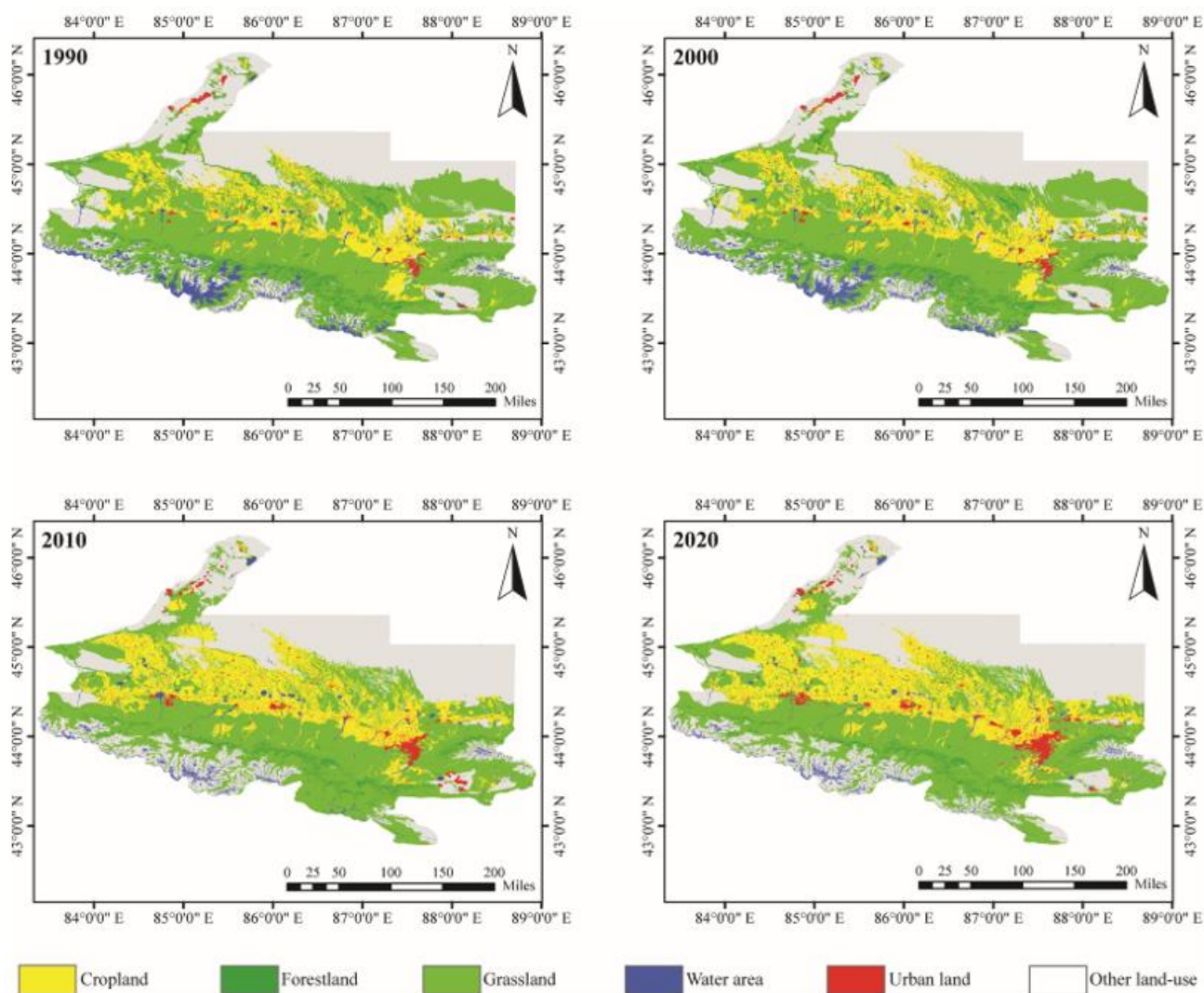


Figure 5. Land use classification maps of the economic belt on the northern slope of Tianshan.

Table 2. Carbon emission coefficients for land-use types.

Land-Use Types	Carbon Emission Coefficient (kg (C)·m <sup>-2</sup> ·a <sup>-1</sup> )	Used in the Study
Cropland	0.0497 [60]	0.0497
Forestland	−0.0645, −0.0527 [60]	−0.0586
Grassland	−0.0021 [60]	−0.0021
Water area	−0.0509, −0.0410 [21]	−0.0459
Other land use	−0.0005 [21]	−0.0005

### 2.4.3. Carbon Emissions from Energy Consumption

Land is an important effecting factor for CEs from energy consumption. Energy consumption is mainly contributed by fuels in urban places, including the sides of factories and transportation. Herein, a total of nine fuel types were taken in account, including three types of coal (crude coal, cleaned coal, and coke), crude coal, four types of oil (gasoline, fuel oil, diesel oil, and kerosene), and two types of gas (liquefied petroleum gas, and natural gas). Based on the existing data [21,60], the equation for calculating CEs from energy consumption was denoted as follows:

$$E_C = \sum E_{Ci} \times f_i \times \frac{M_{CO_2}}{M_C} \tag{2}$$

$$f_i = A_i \times B_i \times C_i, \tag{3}$$

in which  $E_C$  is the total CEs from energy consumption;  $E_{C_i}$  is the consumption amount for fuel  $i$ ;  $f_i$  is CEC for fuel  $i$ ;  $M_{CO_2}/M_C$  is the same with Equation (1); and  $A_i$  indicates the average low calorific value,  $B_i$  represents the unit calorific value carbon content, and  $C_i$  is the carbon oxidation rate of fuel (Table 3). The  $A_i$  and  $C_i$  were acquired from the guidelines for the preparation of provincial greenhouse gas inventories of China [61].

**Table 3.** Required parameters for estimating CEs from energy consumption.

Energy	Average Low Calorific Value (kJ/kg)	Unit Calorific Value Carbon Content (kg/10 <sup>6</sup> KJ)	Carbon Oxidation Rate (%)	Carbon Emission Coefficient (kg/kg)
Coal	20,908	26.37	94%	0.5183
Cleaned coal	26,344	25.41	93%	0.6225
Coke	28,435	29.5	93%	0.7801
Gasoline	43,070	18.9	98%	0.7977
Kerosene	43,070	19.5	98%	0.8231
Diesel oil	42,652	20.2	98%	0.8443
Fuel oil	41,816	21.1	98%	0.8647
Liquefied petroleum gas	50,179	17.2	98%	0.8458
Natural gas	35,585	15.3	99%	0.5390

#### 2.4.4. Carbon Intensity

Accordingly, CI was the amount of CEs per unit of GDP, and the calculation progress is shown in Equation (4):

$$CI = \frac{CE}{GDP} \quad (4)$$

where CI is the carbon intensity; CE represents to the total carbon emission; and GDP indicates the gross domestic product of a particular area. CI in this study referred to the CI from energy consumption.

#### 2.4.5. Spatial Autocorrelation Model

To analyze the association degree between adjacent regions, the spatial autocorrelation method, which could perform further evaluations on the significance, was proven to be a potential approach [62]. With the help of this method, the attribute values between two neighboring spatial units would be calculated and the spatial correlation could be further analyzed. In this way, the agglomeration features for each spatial unit could be analyzed and evaluated [63]. This approach branched into global and local spatial autocorrelation models, and several calculating procedures were proposed, such as Moran's I, Geary's C, Getis, and Join count. Herein, both global and local spatial autocorrelation models were conducted.

#### 2.4.6. Global Spatial Autocorrelation Model

Global Moran's I was introduced as the most conventional statistical test for revealing spatial autocorrelation in the single variable map or in regression residuals [64]. This method was operated to describe the degree of spatial association and significance in published data reports, and the calculation was taken by the following equation [65]:

$$I = \frac{n \sum_{i=1}^n \sum_{j=1}^n w_{ij} [(y_i - \bar{y})(y_j - \bar{y})]}{\sum_{i=1}^n \sum_{j=1}^n w_{ij} \sum_{i=1}^n (y_i - \bar{y})^2} \quad (i \neq j), \quad (5)$$

of which  $y_i$  is the variable of area  $i$  ( $I = 1, 2, 3, \dots, n$ );  $\bar{y}$  represents the average value of all regions, and  $y_j$  is that value of other regions (where  $j \neq i$ ); and while  $W_{ij}$  is the spatial weight matrix (when two regions were topologically adjacent, then  $W_{ij} = 1$ , otherwise  $W_{ij} = 0$ ).

Normally, the range of Moran's I is from  $-1$  to  $1$ . Moreover, if the value is  $>0$ , it indicates that there is a positive spatial autocorrelation between the units, and the  $<0$  value suggests a negative spatial autocorrelation, while if the value Moran's I value is equal

to 0, it illustrates the variable compliance with the stochastic spatial distribution [66]. The smaller the absolute value, the weaker the spatial autocorrelation, and vice versa.

The normalized statistics  $Z(I)$  of the Moran's  $I$  are generally consistent with the normal distribution [67]:

$$Z(I) = \frac{I - E(I)}{\sqrt{\text{VAR}(I)}} \sim N(0, 1). \quad (6)$$

In above formula,  $\text{Var}(I)$  is the theoretical variance of the Moran's  $I$ ;  $E(I) = -1/(n - 1)$  represented as the mean.

#### 2.4.7. Local Spatial Autocorrelation Model

This model is extensively applied for identifying the "hot spots" or "cold spots" in the entire area, and further classification of those spots into different spatial cluster and spatial outliers [67,68]. Local Moran's  $I$  was an indicator for spatial autocorrelation, and could be obtained by following equation:

$$I_i = \frac{(y_i - \bar{y})}{\sigma^2} \left( \sum_{j=1, j \neq i}^n W_{ij} (y_j - \bar{y}) \right), \quad (7)$$

in which  $y_i$  represents the variable of specific region  $i$  ( $i = 1, 2, 3, \dots, n$ ); while  $y_j$  is the variate for other sections (where  $j \neq i$ );  $\bar{y}$  is the average value;  $\sigma^2$  indicates the variance of  $y$ ; and  $W_{ij}$  is the weight matrix normalized by the row (sum of each row is equal to 1).

If a region owned a positive value of local Moran's  $I$ , it suggested a similar or closer value for adjacent areas, and these parts were classified as spatial clusters. Oppositely, a minus value illustrated that these adjacent areas owned relatively diverse values, and were categorized as spatial outliers.

If the local Moran's  $I$  value of an area is high, and that value of the close area is also high, this type of spatial cluster is called a high-high cluster. If that value is low for the specific area and the neighboring sections, this type is called a low-low cluster. For the spatial outlier, if the value is low for an area and the adjacent regions take a high value, this type is named as a high-low cluster; moreover, if the value is low for the selected area and high for the neighboring places, this type is referred to as a low-high cluster. A scatter plot could be obtained after the analysis, and include the calculation results of all areas, while the results of regions that passed the significance test were revealed in LISA cluster maps. Four different quadrants were represented to the four different clusters mentioned above, and the results based on detailed calculations were placed in different quarters. For the LISA cluster map, the principle and organization were the same (four types of regions), and the high-high clusters were known as "hot spots", while low-low clusters were known as "cold spots".

#### 2.4.8. Spatial Carbon Balance Zoning

- Economic contribution coefficient

The economic contribution coefficient (ECC) was applied to evaluate the impartiality of economic contribution within the study area. In this method, the differences in carbon emissions within the area were expressed from an economical aspect, and results could provide scientific instructions for coordinative economic construction and ecological civilization construction [69,70]. ECC is one of the most important indexes for reflecting the carbon emission productivity of the study area, and was calculated by Equation (8):

$$ECC = \frac{G_i}{G} / \frac{C_i}{C}, \quad (8)$$

in which  $G_i$  was the GDP value of a county or an area of NST and  $G$  is the GDP value of NST.  $C_i$  and  $C$  represent the carbon emissions of a county or an area of NST and that of the entire NST, respectively.  $ECC > 1$  represents that the contribution rate of the land-use carbon emissions of area  $i$  was lower than its contribution in economics, which suggests that the economic contribution of carbon emissions was relatively higher [71]; the opposite results suggest the economic contribution of carbon emissions was comparatively lower.

- Ecological support coefficient

Ecological issues from carbon emissions were related with certain externality, and the different carbon sink capacity of an area could affect surrounding counties. Ecological support co-efficient (ESC) could measure the impartiality of ecological carrying capacity, and further reflect the carbon sink capacity of the area [2]. Hence, this method could express the difference in the value of the carbon sink capacity of each studied area, and proper policies on carbon reduction could be proposed based on obtained results. ESC could be calculated by Equation (9):

$$ESC = \frac{C_{Ai}}{C_A} / \frac{C_i}{C} \quad (9)$$

where the  $C_{Ai}$  is the carbon sink of an area in NST, and  $C_A$  was the carbon sink of NST.  $C_i$  and  $C$  represent the carbon emissions of a county or an area of NST and that of the entire NST, respectively.  $ESC > 1$  indicates that the contribution of the carbon sink/carbon absorption of area  $i$  was higher than that of carbon sink/carbon emissions, and has a positive effect on the carbon consumption in NST and related areas [65]. Opposite results suggest a negative effect on the carbon consumption in the study area.

### 3. Results

#### 3.1. Land Use of the Economic Belt on the Northern Slope of Tianshan

Land use of the subject area was analyzed based on data in 1990, 2000, 2010, and 2020. Then, the characteristics of remarkable changes over four decades were analyzed and shown in Table 4. Typical characteristics and alterations were as follows: the grassland, cropland, and the other land use were the most dominant land-use types in this area. In the land-use structure, the grassland was standing at the highest level compared with other types (occupying about 40% of total), while the other land-use types remained to be at the second highest position (possessing the 30% of entirety). The cropland was considered as one of the major types with its proportion about over 10% of land use. Forestland, water area, and urban land-use types were observed with a relatively lower ratio (about 3%) compared to that of other types mentioned in this work.

**Table 4.** Land-use data of six land-use types in the economic belt on the northern slope of the Tianshan urban agglomeration in 1990, 2000, 2010, and 2020.

Year	Unit	Cropland	Forestland	Grassland	Water Area	Urban Land	Other Land-Use
1990	Area(km <sup>2</sup> )	10,823.2586	4091.672508	41,313.574668	3408.190828	1094.109508	28,988.061512
	proportion	12.36%	4.76%	47.18%	3.89%	1.25%	33.12%
2000	Area(km <sup>2</sup> )	11,565.984052	4052.581704	39,980.095328	3512.172556	1329.544792	28,391.498704
	proportion	13.3%	4.62%	45.66%	4.01%	1.52%	32.43%
2010	Area(km <sup>2</sup> )	16,557.012452	1832.383800	37,130.093472	1832.715896	1812.855208	27,115.840240
	proportion	18.91%	2.09%	42.41%	2.09%	2.07%	30.97%
2020	Area(km <sup>2</sup> )	17,758.219364	1766.574900	34,869.092688	1722.349804	2452.276364	26,825.591624
	proportion	20.28%	2.02%	39.82%	1.97%	2.8%	30.64%
1990–2020	Area of change	6934.9606	−2325.097608	−6444.48198	−685.841024	1358.166856	−2162.469888
	change rate	64.07%	−56.82%	−15.60%	−49.46%	124.13%	−7.45%

Analyses on the dynamic degrees of the changes and changing trends for each land type were conducted. Grassland owned 47.18% in the land-use structure in 1990 and showed a gradually decreased trend (value of 39.82% in 2020), and the dynamic degree was −7.36% in the selected time period. The same phenomenon was observed for other land-use types. Compared with the 33.12% in 1990, the ratio descended to 30.64 in 2020 for the other land-use types, and its dynamic degree was −2.48%. In the 1990 to 2000 sections, the percentages of cropland were 12.63% and 13.3%, suggesting a slight arising, and the value ascended to 20.28% in 2020, which illustrated a remarkable increase with the dynamic degree of 7.65%. The dynamic degree for forestland, water area, and urban land were calculated, and resulted as −2.74%, −1.8%, and 1.55%, respectively. Dynamic degrees analysis revealed the changes in land-use types of the study area in the recent

30 years, in which the cropland and urban land showed increasing trends, while decreasing trends were observed from the other four land-use types. It was worth mentioning that the changing rates of urban land and cropland, which were the main contributors for carbon emissions, were obviously higher than other land-use types.

### 3.2. Characteristics of Carbon Emissions of the Economic Belt on the Northern Slope of Tianshan

After data processing, carbon emissions from land uses, carbon absorptions (CAs) from each of the land-use types, total CEs, total CAs, and net carbon emissions (NCEs) were calculated and analyzed for different time period (Table 5). According to the published works on the division of contributing factors for CEs and CAs [43], among the land-use types, cropland and urban land were mainly contributing factors for CEs, while the other four types were referred for CAs contributors.

**Table 5.** Land-use specific carbon emissions and carbon absorptions.

Year	Land-Use-Specific Carbon Emission/Absorptions (10 <sup>4</sup> t)						Total Carbon Emissions	Total Carbon Absorptions	Net Carbon Emissions
	Cropland	Forestland	Grassland	Water Area	Urban Land	Other Land Use			
1990	197.236 6.53%	−87.916 48.20%	−31.811 17.44%	−57.360 31.45%	2821.76 93.47%	−5.314 2.91%	3018.996 100.00%	−182.401 100.00%	2836.595
2000	210.771 6.34%	−87.076 47.53%	−30.785 16.81%	−60.120 32.82%	3114.75 93.66%	−5.205 2.84%	3325.521 100.00%	−183.186 100.00%	3142.335
2010	301.724 2.6%	−39.372 37.94%	−28.59 27.55%	−30.845 29.72%	11,297.76 97.4%	−4.971 4.79%	11,599.484 100.00%	−103.778 100.00%	11,495.706
2020	323.611 0.97%	−37.958 38.45%	−26.849 27.20%	−28.987 29.37%	32,897.53 99.03%	−4.918 4.98%	33,221.141 100.00%	−98.712 100.00%	33,122.429

In Table 5, the plus values represent carbon emissions, while minus values represent the carbon absorptions. In four decades of time, the total NCE in the area increased significantly from  $30.19 \times 10^6$  t to  $332.11 \times 10^6$  t, which raised by about 11 times. The data show a slightly raising trend between 1990 and 2000, and a rapid growth trend during the second ten-year period (2000–2010), and the tendency is still obvious for the last ten-year period. Among land-use types, the cropland and the urban land were observed to be the main factors for CEs, while the forestland, grassland, water area, and other land-use types appeared to be contributors for carbon absorption. During the selected period, the contribution rates for urban land were 93.47%, 93.66%, 97.4%, and 99.03%, respectively. This showed that nearly all the CEs were contributed by urban land use. Comparatively, the carbon absorption amount of forestland was increasing slowly, which meant the canceling efficiency of CEs of forestland by its carbon absorption became relatively faint.

#### 3.2.1. Temporal Characteristics

The carbon emission, carbon absorption, and net carbon emission of 12 different units were calculated by the Equations (1)–(3) based on the land use and energy consumption data. It could be seen from Figure 5 that the cropland and the urban land were considered as carbon sources, whereas the forestland, the grassland, the water area, and the unused land appeared to be carbon sinks. Hence, total CEs correspond to the sum of urban land and cropland, while the sum of CAs of the other four types were called the total CAs. The NCEs were the sum of CEs and CAs.

Results illustrate that the NCE of the studied area was increasing, and the increasing trend and progresses were relatively different for each individual region (Figure 6A). In 1990, the rank for annual increasing degree was as follows: Urumqi > Changji > Karamay > Kuitun > Usu > Manas > Shihezi > Fukang > Hutubi > Dushanzi > Shawan. Nevertheless, in 2020, the rank was as follows: Shihezi > Urumqi > Karamay > Changji > Kuitun > Manas > Usu > Hutubi > Shawan > Fukang > Dushanzi. Among them, the NCE of Urumqi, Shihezi, Changji, and Karamay cities possessed a relatively higher speed of growth, such as the NCE of Urumqi, which was  $12.57 \times 10^6$  t in 1990 and increased to  $78.86 \times 10^6$  t in 2020

(about 6 times); NCE for Shihezi in 1990 was  $0.73.59 \times 10^4$  t, and rose to  $79.79 \times 10^6$  t in 2020 (about over 100 times); and that of Changji increased from  $6.03 \times 10^5$  t to  $44.60 \times 10^6$  t in 30 years (about 7 times). It can be seen from the data analysis that the speed could reach over 100 times in the most significantly increased regions.

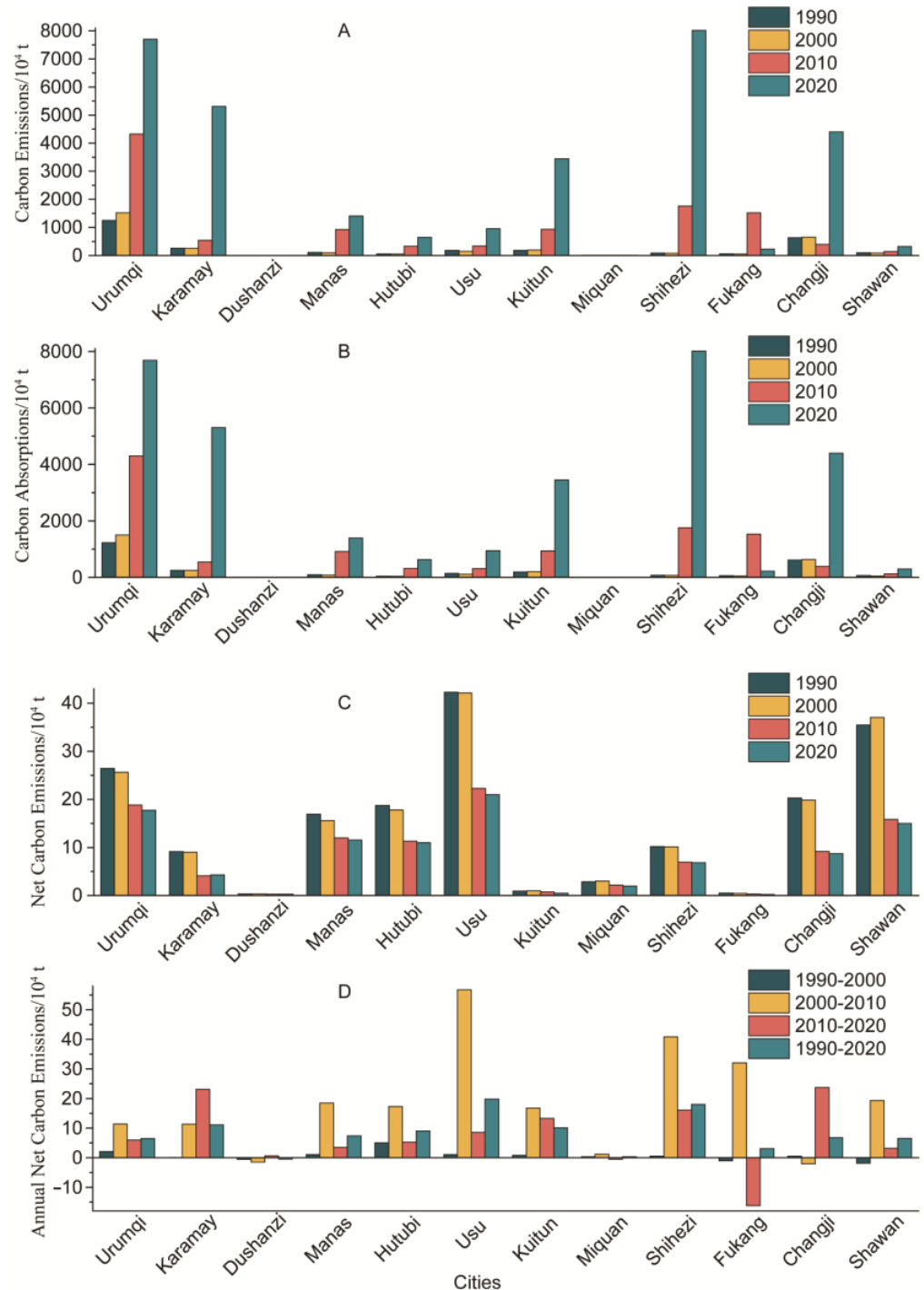
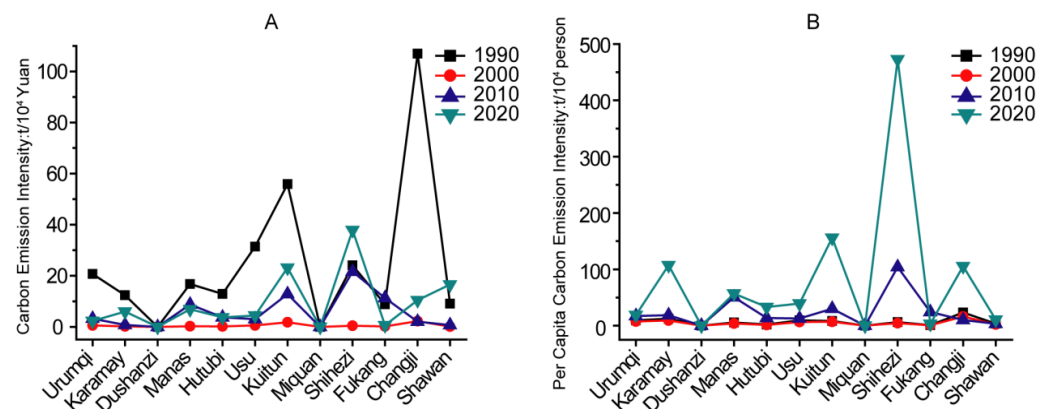


Figure 6. Carbon emissions (A), carbon absorptions (B), net carbon emissions (C), and annual net carbon emissions (D) of the economic belt on the northern slope of Tianshan in 1990, 2000, 2010, and 2020.

Carbon absorption of the study area increased noticeably during a 30-year time period. Among them, CAs of Urumqi, Shihezi, Karamay, and Changji were higher than others, while that of Dushanzi, Miqan, and Shawan were relatively lower (Figure 6B). However, net carbon emissions decreased in different degrees between 1990 and 2020. NCEs of Usu, Shawan had the highest values in 1990 compared with other areas (Figure 6C). The result of the annual net carbon emissions revealed that the ANCEs of the area took comparatively lower value in 1990–2000, while the highest value of that was in 2000–2010, and changes were non-significant during 2010 to 2020 (Figure 6D).

The result of the analysis on the carbon intensity from energy consumption is visualized in Figure 7A. Outcomes revealed that CI was decreased remarkably. The highest level of CI was observed in Changji in 1990 (about  $100 \text{ t}/10^4 \text{ yuan}$ ), while Kuitun was the second highest with the value at about  $55 \text{ t}/10^4 \text{ yuan}$ . However, the CIs were declined evidently in 2020, and a relatively higher quantity of that was calculated from the data of Shihezi (about  $35 \text{ t}/10^4 \text{ yuan}$ ). However, the per capita carbon emission intensity (PCCEI) revealed an increasing trend during the study period (Figure 7B), and the trend became more obvious from 2010. A rapid increase was observed in Shihezi from about  $2 \text{ t}/10^4 \text{ person}$  in 1990 to  $470 \text{ t}/10^4 \text{ person}$  in 2020, and relatively noticeably raised values were obtained from Karamay (about  $100 \text{ t}/10^4 \text{ person}$ ), Manas (about  $50 \text{ t}/10^4 \text{ person}$ ), Kuitun (about  $150 \text{ t}/10^4 \text{ person}$ ), and Changji (about  $110 \text{ t}/10^4 \text{ person}$ ) cities as well in 2020.



**Figure 7.** Carbon emissions of energy consumption (A) and per capita carbon emissions (B) of the economic belt on the northern slope of Tianshan.

### 3.2.2. Spatial Characteristics

Twelve cities in the NST were classified into different levels according to the analysis on net carbon emissions and carbon intensities, and are presented in Figures 8 and 9, respectively. In 30 years, Urumqi was considered to possess the highest NCEs of all the subjected places, whereas Changji and Karamay also possessed relatively higher NCEs than other cities. In 1990, Urumqi, Karamay and Changji showed higher NCEs (up to  $12 \times 10^6 \text{ t}$ ), while other cities took values between  $1 \times 10^5$  and  $2 \times 10^6 \text{ t}$ . The spatial difference appeared to be reduced gradually, and took values of 0–1. Nevertheless, higher results were obtained during the period of 2010–2020 for Urumqi, Shihezi, Changji, Manas, Kuitun, and Karamay (about  $50\text{--}80 \times 10^6 \text{ t}$ ), while the NCE intensities of other places were at the range of  $0\text{--}50 \times 10^6 \text{ t}$ . Above results suggest a lower NCEs level of the whole area. Carbon intensities of NST had the highest level in 1990, in which Changji, Usu, and Kuitun had the value between 30 and  $110 \text{ t}/10^4 \text{ yuan}$ . However, the CI had the lowest value ( $0\text{--}10 \text{ t}/10^4 \text{ yuan}$ ) in 2000. Moreover, CI was rising in height from 2010, and Shihezi, Kuitun, and Fukang had the fastest ascent speed.

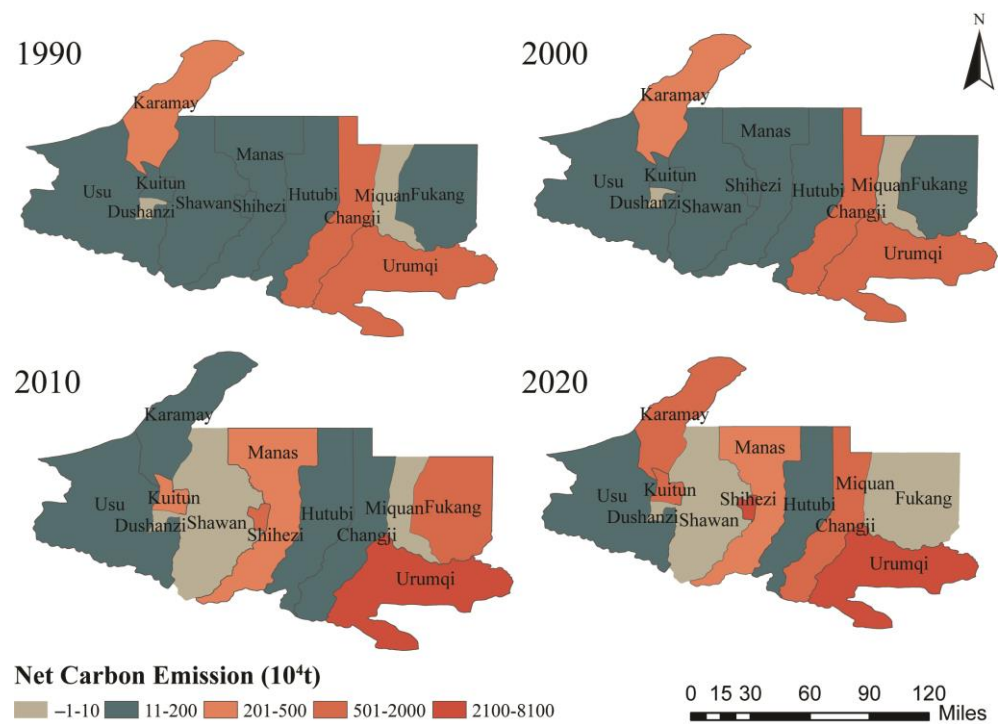


Figure 8. Net carbon emissions of the economic belt on the northern slope of Tianshan.

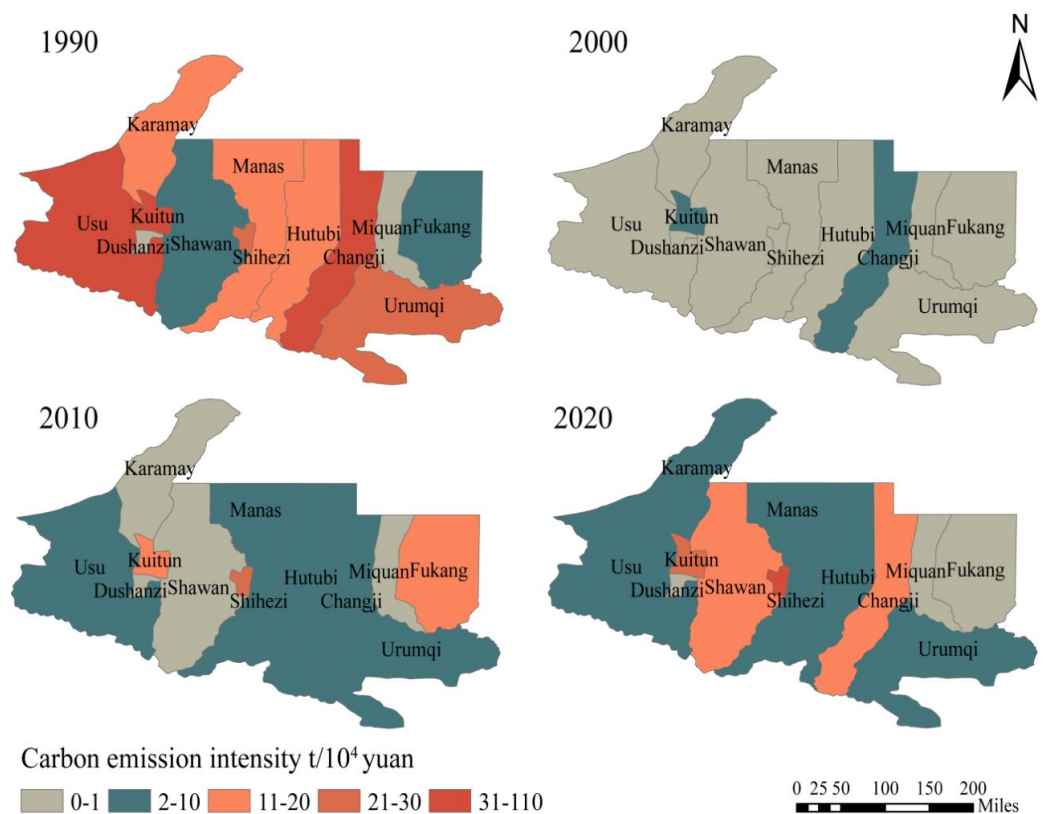


Figure 9. Carbon intensities of the economic belt on the northern slope of Tianshan.

### 3.3. Spatial Correlation of Carbon Emissions and Carbon Intensity

The Global Moran's I and Z(I) of the NCEs and CIs were processed and calculated in ArcGIS10.2 software, and the results are shown in Table 6. It was revealed from the outcomes that Moran's I for NCEs > 0 from 1990 to 2020 and the Z values were fluctuating. However, none of those values were passed from the significance test, which illustrated

a possibility that there was no obvious positive spatial correlation among the selected cities in the studied area, meanwhile, this also proposed that there might be a negative spatial correlation. The Moran's I value of the NCEs gradually became smaller for the research period, which indicated that the spatial correlation between the selected units had a declining trend and tended to have a random distribution. Moran's I values of the NCEs intensity were  $<0$ , and the Z values were also  $<0$  during the period of 1990–2000. Despite the fact that Moran's I value  $>0$  was obtained for 2010–2020, none of these values passed the significance test. Accordingly, it was tentatively concluded that spatial correlations between selected cities in the NST were less evident; meanwhile, neither an obvious "cold spot" nor "hot spot" was confirmed by the data analysis.

**Table 6.** The moran's I values and Z values of selected time period.

Year	1990	2000	2010	2020	1990	2000	2010	2020
Moran's I	−0.008	−0.005	−0.004	−0.242	−0.250	−0.255	0.099	0.076
Z(I)	0.5433	0.631	0.2855	−0.7371	−1.0878	−0.979	0.0447	1.0281

The correlation between the land-use NCEs and CIs from energy consumption was analyzed by the LISA method, and results were obtained by processing with ArcGIS10.2 and GeoDa software (v1.12) (Figure 10). In this analysis, Miqan was a "cold spot" during 1990–2000, which illustrated that the total CEs of this city were lower than other regions. Miqan is a relatively new city built in 2007. The population density of this city was relatively lower, and was considered as a place in the early stage of development. Hence, the NCEs level was comparatively lower. Moreover, less spatial variation was revealed from this region, and a spatial aggregation mode was confirmed to be possessed by this area. LISA analysis on CE intensity from energy consumptions did not show any "cold/hot spot" in the period of 1990–2000, while Fukang City could be considered as a "cold spot" in 2020.

### 3.4. Spatial Carbon Balance Zoning Analysis

The results of the economic contribution coefficient (ECC) are shown in Figure 11. The ECCs of each unit in NST were remarkably different, and regional differences were also obvious, in which Urumqi possessed a relatively higher ECC value at 3.93 in 1990 and 9.24 in 2020. Urumqi is a capital city of Xinjiang province, which contains a large amount of economic entities, and its GDP remained to the highest in the region. The ECC of Miqan was raised from 2.21 to 8.68 between 1990 and 2020, and revealed a fluctuated elevation in economic contribution. Further analysis of ECC indicated a relatively unbalanced economic contribution of carbon emissions for cities in NST during the study period. In 1990, two investigated areas (Kuitun and Changji) had ECC values between 0 and 2, six of them (Usu, Dushanzi, Manas, Hutubi, Miqan, and Urumqi) had values from 2 to 4, and four (Karamay, Shawan, Shihezi, and Fukang) had values of 5–7. However, in 2020, there were four regions (Kuitun, Shawan, Shihezi, and Fukang) that had ECCs between 0 and 2, four (Usu, Karamay, Manas, and Changji) revealed values between 2 and 4, Hutubi had the value between 5 and 7, and three (Urumqi, Miqan, Dushanzi) showed ECCs between 8 and 12.

Analysis revealed relatively lower values of ecological support coefficients (ESC) of investigated area, and no significant regional differences were observed (Figure 12). In 1990, there were seven regions that took ESC values between 0.0 and 2.0, three had ESCs from 2.1 to 4.0, and two had that value at 4.1 to 7.0. In 2020, Manas had the ESC value of 7.4, six regions (Karamay, Kuitun, Shawan, Shihezi, Changji, and Urumqi) had values between 0.0 and 2.0, ESC values of four regions (Usu, Dushanzi, Hutubi, and Miqan) were from 2.1 to 4.0, and Fukang had the value of 5.5. These results indicate that there were no remarkable spatial differences in ESCs, which reveals that the carbon absorption ratio was smaller than the carbon emission ratio.

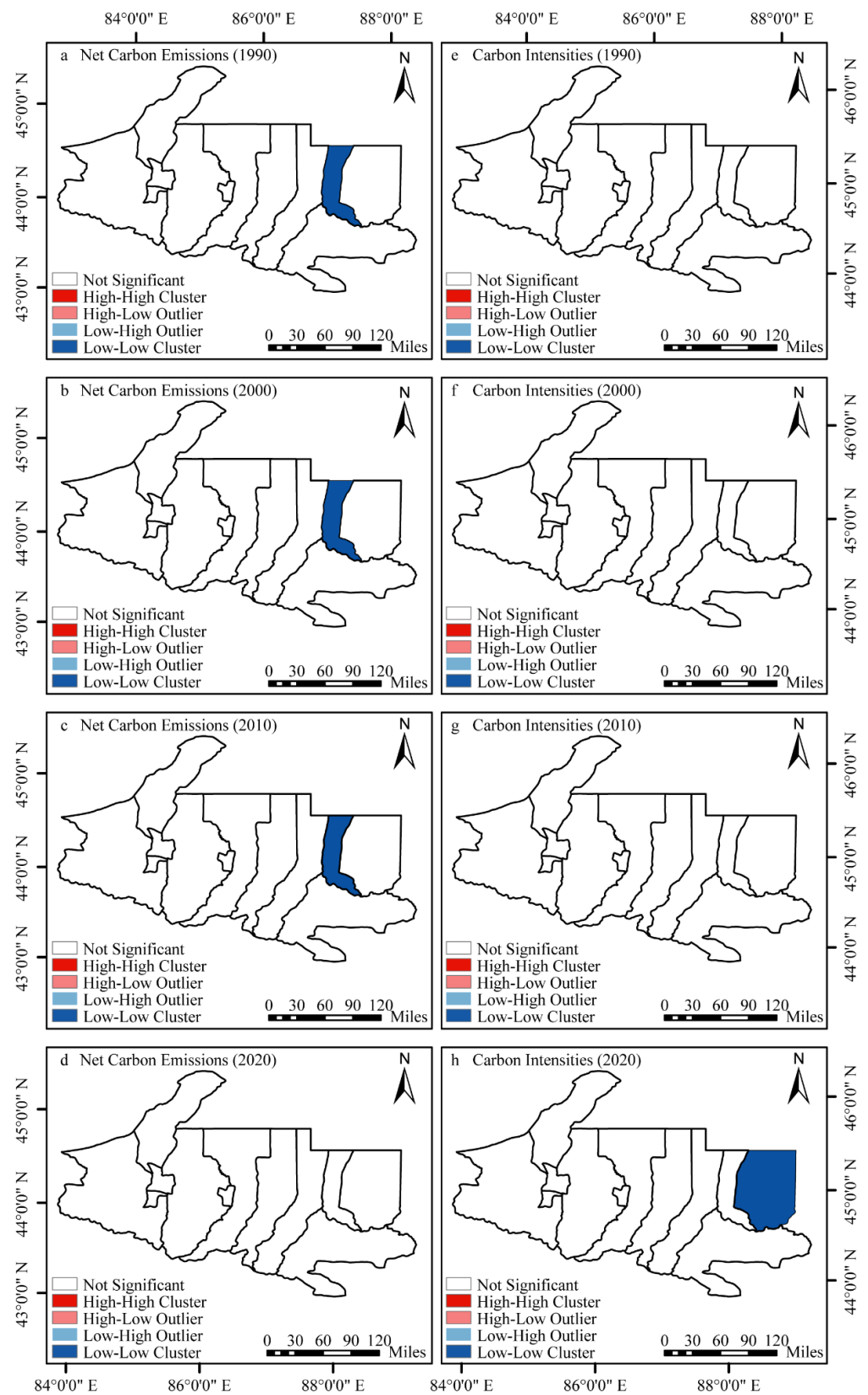


**Figure 10.** LISA cluster maps of net carbon emissions (a–d) and carbon intensities (e–h) for the economic belt on the northern slope of Tianshan in 1990, 2000, 2010, and 2020.

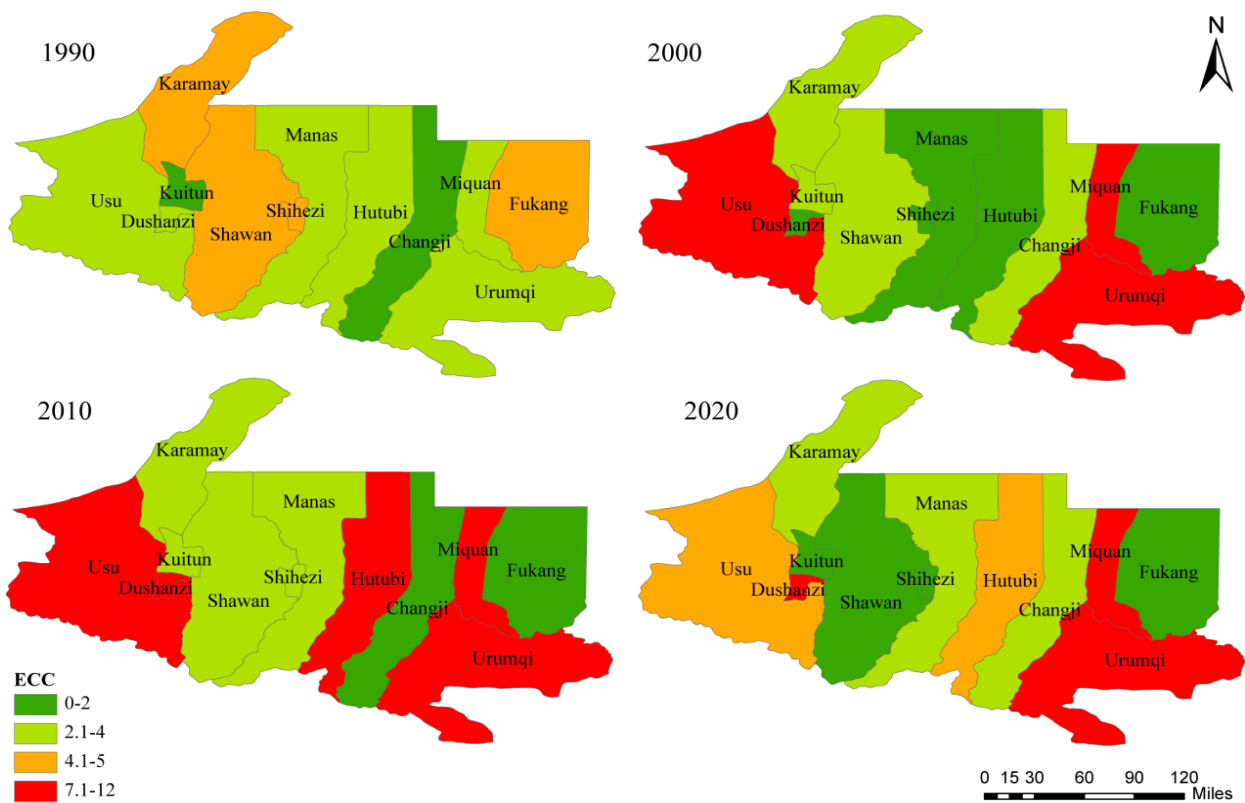


Figure 11. Spatial distribution of economic contribution coefficient of the economic belt on the northern slope of Tianshan in 1990, 2000, 2010, and 2020.

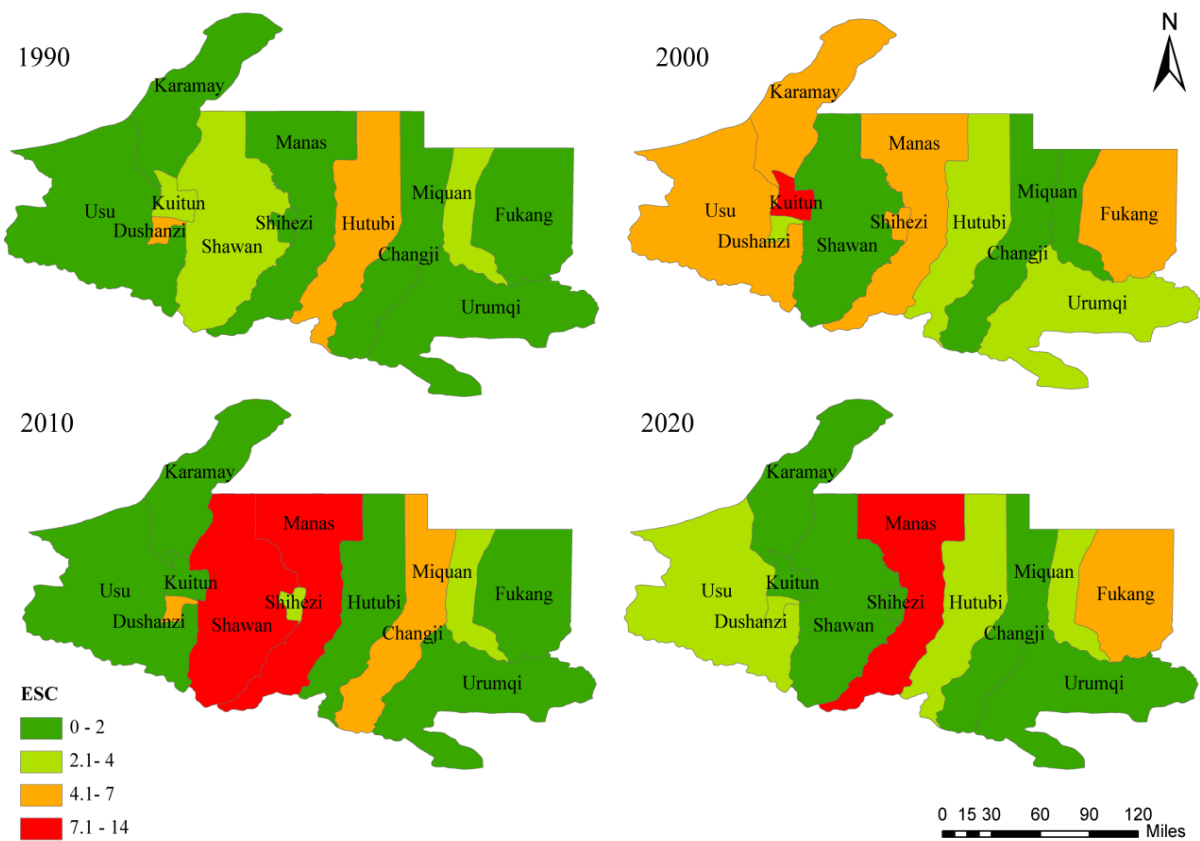


Figure 12. Spatial distribution of ecological support coefficient of the economic belt on the northern slope of Tianshan in 1990, 2000, 2010, and 2020.

### 3.5. Spatial Carbon Balance Division of the Economic Belt on the Northern Slope of Tianshan

The net carbon emissions of NST had a close relationship with energy consumption, economic development, and land use of the area. According to the ECCs, ESCs, and NCEs of investigated area during study period, the spatial carbon balances were divided into four levels, including carbon sink functional areas, low-carbon economic areas, carbon intensity control areas, and high-carbon optimization areas, respectively. Detailed characteristics and information are shown in Table 7.

**Table 7.** Characteristics of carbon balance zoning.

Carbon Balance Zoning	Division Bases	Zoning Characteristics
Carbon sink functional areas	$ECC > 1, ESC > 1, C_A > C_i$	Higher ECC and ESC, $C_A$ is higher than $C_i$ , possess carbon sink function and carbon sequestration capacity
Low-carbon economic areas	$ECC > 1, ESC > 1, C_A < C_i$	Higher ECC and ESC, $C_A$ is lower than $C_i$ , lower NCE
Carbon intensity control areas	$ECC > 1, ESC < 1, C_A < C_i$	Higher ECC, and lower ESC, $C_A$ is lower than $C_i$ , higher NCE
High-carbon optimization areas	$ECC < 1, ESC < 1, C_A < C_i$	Extremely higher NCE, lower ECC and ESC

Note:  $C_A$  was carbon absorption,  $C_i$  was carbon emission.

Analytical results of spatial carbon balance division based on the above zoning rules are described in Figure 13. In the first 10 years (1990–2000), Dushanzi belonged to carbon sink functional areas, and all the other units appeared to be low-carbon economic areas. In the second 10-year period (2000–2010), Urumqi, Kuitun, and Fukang were revealed as carbon intensity control areas, Dushanzi was divided into carbon sink functional areas, and the other eight regions were considered to be low-carbon economic areas. In the third 10 years (2010–2020), five regions, including Manas, Hutubi, Usu, Miqan, and Fukang, were divided into low-carbon economic areas, Dushanzi remained a carbon sink functional area, and the other six (Urumqi, Karamay, Kuitun, Shihezi, Shawan, and, Changji) were considered as high-carbon optimization areas.

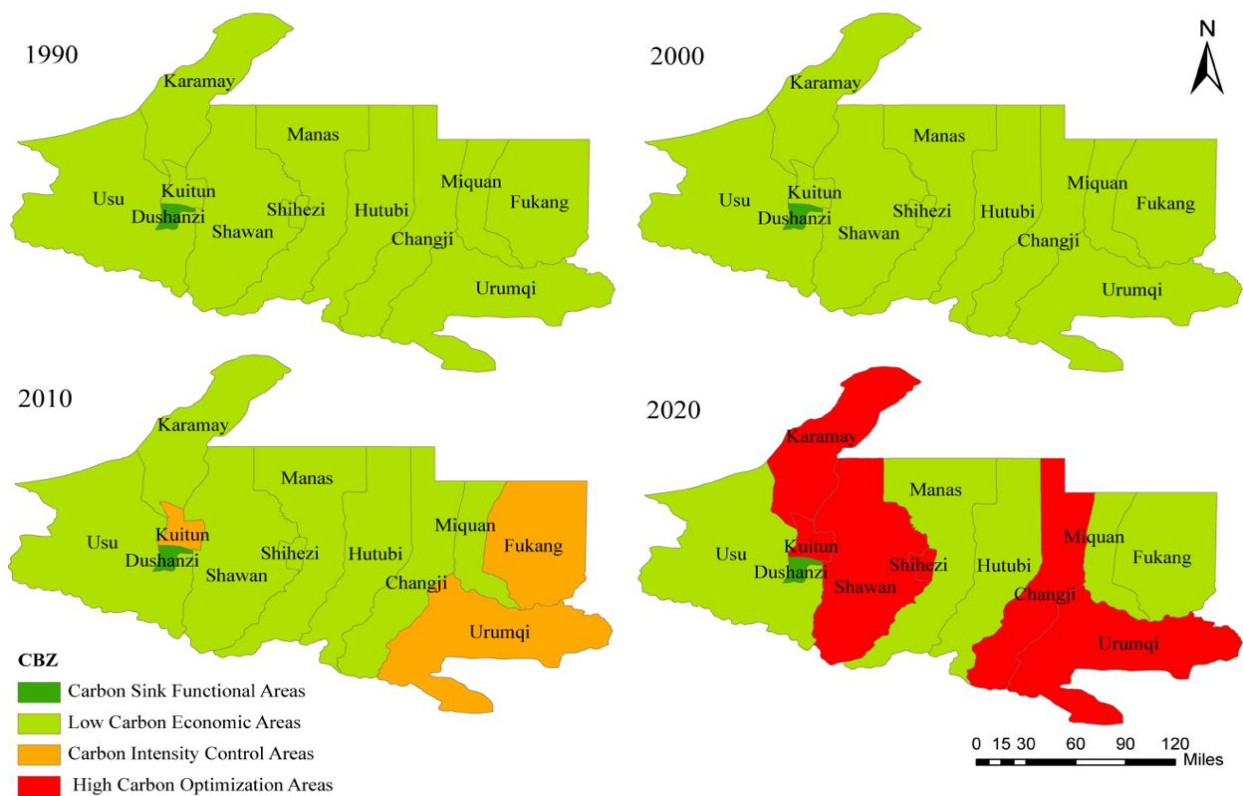


**Figure 13.** Carbon balance zoning of the economic belt on the northern slope of Tianshan in 1990, 2000, 2010, and 2020.

## 4. Interpretation and Discussion

In this work, land-use information was obtained from multi-temporal Landsat images with the help of random forest classification. Meanwhile, land-use carbon emissions for a selected time period were acquired and estimated by data processing. Furthermore, land-use characteristics, and spatial correlation of net carbon emissions and carbon intensities were calculated and analyzed. In this part, results were interpreted, and their implications were tentatively discussed.

### 4.1. Characteristics of Land Use, Carbon Sources, and Carbon Sinks

The land-use analysis based on multi-temporal land cover/use mapping revealed a remarkably expanding trend for urban land and cropland in the study area during the total research period. However, sharp decreased phenomenon was observed from the forestland and water area. Reasons for such changes were analyzed. As the most developed agricultural area in the province, a promising potential for agriculture was observed from the vast territory and the rich water sources of this area [47]. Moreover, with the continuous escalation of population, the need for crops and other agriculture-related products increased remarkably [48]. Consequently, the scope of the cropland was expended extremely. As a core point for the economic strategy of the whole of Xinjiang, and especially one of the center regions for the “belt and road” strategy, there were tremendous requirements for the economic development [52]. Thus, the unparalleled industrialization and urbanization, leading to the growth of a number of cities and industrial areas, brought a huge increase in urban land use. Accordingly, the above expansions were benefited mainly from the series conversion of forestland, water area, and the unused land.

Remarkable changes in land use directly influenced carbon emissions. For instance, the changing ratio of urban land went from 1.25% to 124.13% during the study period, while CEs increased from 95.58% to 98.76%, which was the most dominant in all land-use types. Meanwhile, the increasing speed of CEs was much slower than that of urban land. These outcomes illustrated that the ascent of area could affect the change in CEs, yet, could not be the main reason for that. The analysis on different aspects pointed out that the increases in construction, industry, and the transportation by the growing population was the main reason. An obvious increasing trend in population density was observed for all the cities in the region in 30 years. The need for consumption of daily products, such as food, housing, clothing, and transportation, was accordingly increased with the great number of humans.

Most of the CEs were originated by urban land, and these results are compliant with the previous results of other studied areas in China or different countries [42]. Four types of land use (forestland, grassland, water area, and unused land) were contributing to the absorption of CO<sub>2</sub>; however, there was significant decreasing in their areas. These results reveal an unbalanced trend between CEs and carbon absorption, which suggests that the rising ratio of CEs was obviously greater than the increase in carbon absorption in the study area.

According to the above analysis, CE reduction of this area should be considered from the following aspects: firstly, CEs from urban and cropland must be controlled; secondly, the unreasonable developments and reductions in the forestland, water area, grassland, and unused land should be noticed and stopped. Therefore, the key point for reducing CEs might be maintaining and gradually increasing forestland, and efficiently controlling the CE amounts from urban land, which suggests the importance of efficient management of the CEs for energy consumption. It was noteworthy that optimizing land-use management and structure could affect positively CE reduction. Nevertheless, as a core economic area, it seems difficult to control the greenhouse gas by slowing the economic development down. However, related policies and implements are strongly demanded for sustainable and environmentally friendly development of this area.

#### 4.2. Characteristics of Carbon Emissions and Carbon Intensities

Urumqi City had the highest carbon emissions during the whole study period; meanwhile, Shihezi possessed the highest speed at net carbon emissions. Changji and Karamay showed rapidly increased NCEs. The main reasons for these increases could be the expanding of the numbers and scope of industrial areas, growth of population density, and development of transportation, which were the main sources of greenhouse gas.

In one aspect, during the urbanization progress, especially under the rapid economic development, an enormous need for energy was required as a fundamental base for industry. On the other hand, the CE intensity was relatively strong, due to deficiencies in technology, insufficient rationality of economics, and high dependency on disposable energy sources. However, the energy efficiency was improved gradually, along with the development of new technologies, and the CE intensity was reduced. A growing trend for per capita CEs was observed, and this phenomenon was remarkable in Karamay City. Per capita CEs for Shihezi remained to be supreme compared to other regions. The urban area of Shihezi is relatively small and densely populated; furthermore, the plant coverage degree was also noticeably lower. These characteristics resulted in a weak carbon sink effect, and thus, the carried CE amount was comparatively more for each unit area.

Shihezi and Changji appeared to be strong CE intensity areas, especially in 1990. The main reasons for that were analyzed as follows: the above regions were considered to be key developing cities for the province, and they closely neighbor Urumqi [53]. Under the integration of the Urumqi and Changji strategy, the industrial development of Changji was greatly accelerated [51]. Shihezi is a new military reclamation city, and is also one of key developing cities. Excessive human activities, such as dense population, transportation, industrial pollutions, and the lack of plan coverage, caused a high carbon intensity. It is worth mentioning that these two cities are in a transforming period, and hopefully, changes in development could decrease the CEs intensity. Urumqi, Karamay, and Kuitun were the cities with a property of high CEs and low CE intensity. Urumqi is an emerging city with rapid development. With a better geographical conditions and convenient transportation with natural resources, this city became one of the core places in the western regions of China, and also became the center of the economy and business of Xinjiang [72]. Urumqi formed an industrial cluster of 10 big industrial aspects, including petrification, construction materials, medicine, food, and other industries. In addition, Karamay is an industrial city, which mainly developed petroleum and related industry. People of Karamay are mainly consistent with a non-agricultural population, and thus the secondary and serve sector industries were comparatively well developed. Analysis suggested that these cities were all developing with a rapid speed compared to other places around, and thus appeared as a strong CEs-weak CEs intensity type.

#### 4.3. Spatial Auto Correlation of Carbon Emissions and Carbon Intensities

The Moran's I analysis illustrated negative spatial autocorrelations between cities in the northern slope of Tianshan Mountain. The Moran scatter plots were mostly located on the LL and L-H quadrant, and this was in accordance with the grading of NCEs. NCEs of several cities were all relatively higher, and some of them appeared with the highest levels of carbon emissions. These results show that low-value and low-high value clusters were comparatively remarkable in the study period.

Previous studies proved that economic expanding could have a positive effect on carbon emissions [35,39]. Miqan city was proven to be a "cold" city for the period of 1990–2010; meanwhile, it was observed from the LISA cluster that Fukang City was a typical "cold" city in 2020. The reasons were analyzed as follows: Miqan was a new established city in this region, and also an under-developing area with less dense population. Additionally, this city possessed a relatively implicit spatial difference, and on a remarkable spatial aggregation. Fukang City was a main industrial city for this region. However, the economic and industrial structure of Fukang was adjusted and upgraded with certain

efforts by local government. These upgrades mainly aim for less energy dependence and strongly pursue the new and higher technologies.

#### *4.4. Spatial Carbon Balance Zoning and Division Analysis*

Spatial carbon balance zoning analysis revealed an unbalanced trend for the whole area, and these phenomena appeared to be more remarkable with the timeline. It was suggested from the analysis that the relationship between economic development and environmental protection could be harmonized by the transformation of economic development mode, which could also improve the ecological pressure of carbon emission. Total evaluation for NST showed that the number of low-carbon economic areas was relatively abundant, and the total CAs was barely sufficient for the entire CEs from energy consumption. Future policies and works could focus to enhance the protections on carbon sink function. Moreover, the number of high-carbon optimization areas was rising with the timeline, and economic contributions were greater than the contributions of land-use carbon emissions. Nevertheless, the carbon sequestration capacity was relatively insufficient, and the total NCEs increased continuously. Recent policies and developing trends pointed out the importance of carbon sink functional areas. It is important to ensure ecological constructions while developing economic constructions. Moreover, future developments should give consideration to the sustainable development of economy and ecology.

#### *4.5. Contributions of Research Findings and Improving Management*

This study conducted the analysis on land-use characteristics and carbon emissions of NST using Landsat remote sensing images and socio-economic statistical data. Moreover, the carbon balance and spatial autocorrelation between carbon emissions and carbon intensities were also investigated with Moran's I model. Current states of carbon emissions and carbon intensity could be investigated to some extent with applied calculation and estimation methods, and the impact of CEs on neighboring cities and adjacent areas was also analyzed. Land-use patterns of NST greatly affected the regional development and ecological environment, and the rapid urbanization and industrialization could lead to an unstable carbon balance. Thus, improving polices should fully take the urban landscape patterns under consideration, and the carbon sink land-use types should be increased, while the land-use types with CEs should be reduced. In addition, energy consumptions in urban land were also a main source of CEs, and the ecological constructions while developing the economic constructions should be considered for the regional development planning.

### **5. Limitations**

This study took analysis of the characteristics of land-use carbon emissions in the subject area, and intended to make some efforts toward the improvement of land-use transitions and carbon metabolism. Hopefully, the methods applied in this work were also applicable in a Chinese context. However, some points should be considered carefully and taken as caution: (1) Though we tried our best to collect the socio-economic statistical data fully, this process was particularly challenging for the locations that lacked energy consumption statistics in the year book. Thus, collected and applied data were hardly considered as the full and accurate source for carbon emission estimation, due to the difficulties and limitation of acquisition from data sources. It was relatively hard to find the acquired data completely, and thus, some data were taken at the value of 0. However, real values of carbon emissions in this area were possibly higher than that of our calculation in this work. (2) The constant data, such as carbon emission coefficients for different land types, were obtained from previous reports. Further studies and investigations are required for improving the accuracy of these parameters.

## 6. Conclusions

In this article, the characteristics of the land-use carbon emissions of the northern slope of the Tianshan Mountain were investigated. We focused on the calculation of carbon emissions based on remote sensing data for a 30-year period, and initially analyzed the current changes and trends of carbon emissions for six types of land uses. Furthermore, the spatial autocorrelation of carbon emissions and net carbon emissions were investigated by applying global Moran's I statistics. The main conclusions are summarized as follows.

- (1) There were significant changes in land use in the study area in 30 years, and the urbanization speed was significantly accelerated by the development of economy. Urban land and cropland were expanding rapidly, while the forestland, grassland, water area, and unused land were decreased remarkably. In addition, urban land was the most dominant contributor for carbon emissions, and it was found that carbon emissions from land use increased significantly over the time period. Policies and adjustments of the land use changing, which are beneficial for carbon balance, should be considered and executed.
- (2) Carbon emissions of NST were remarkably rising, and the carbon intensities were also higher. Urumqi had the highest carbon emissions during the whole study period; meanwhile, Shihezi possessed a highest speed in net carbon emission (NCE). Changji and Karamay showed a rapidly increased NCE. Thus, carbon emissions of this area should be controlled efficiently. Moreover, the industrial and urban development should be controlled and adjusted for the sustainable and environmentally friendly development.
- (3) The increasing ratio of the carbon intensities of Kuitun, Karamay, and Changji City were significantly higher than that of other cities, and these phenomena might be caused by a rapid increase in population and developments in industry. Policies should be considered for the economic development mode and other sides related to carbon intensities.
- (4) Based on the carbon balance zoning analysis and related indexes, NST was divided into four areas, which were carbon sink functional areas, low-carbon economic areas, carbon intensity control areas, and high-carbon optimization areas, respectively. Among the study region, the numbers of low-carbon economic areas were relatively abundant, which suggested that the amount of carbon absorptions were insufficient to eliminate the carbon emissions from energy consumption. Thus, future countermeasures should focus on the protection of the carbon sink functions of the area. However, analysis indicated that the number of high-carbon optimization areas was increasing with the timeline, and economic contributions were considerably higher than the contribution of land-use carbon emissions. Furthermore, the carbon sequestration capacity was insufficient, and total net carbon emissions were increasing. Policies related to eco-friendly and environmentally friendly development also embodied the importance of carbon sink function; and thus, future developments should consider the ecological constructions while developing the economic constructions in order to guarantee sustainable development in both economy and ecology.

In conclusion, carbon emissions in this area increased noticeably, and should be regulated strictly. The economic and industrial structure of the region had a great demand to be adjusted and optimized, and gradually reached to a low-carbon economy state. This study could provide some references to deeper understandings of the characteristics of land-use carbon emissions of the northern slope of Tianshan Mountain. Analysis could offer some useful insights into the development of reduction policies and methods of sustainable and low-carbon development of the area. Furthermore, the applied method and model in this study could be a promising protocol to better understand the carbon emissions analysis of the areas, the CEs of which were mainly impacted by land-use changes, energy consumptions, and economic growth, such as the urban agglomeration of the Pearl River Delta, middle reaches of the Yangtze River, and Chengdu-Chongqing (CC) urban agglomerations.

**Supplementary Materials:** The following supporting information can be downloaded at: <https://www.mdpi.com/article/10.3390/su151511778/s1>, Table S1. Total energy consumptions of 12 selected regions in northern slope of Tianshan mountain (Total consumptions/104 t). Table S2. Per capita Gross Domestic Product value of 12 selected regions in northern slope of Tianshan mountain in 1990, 2000, 2010 and 2020 (103 CNY). Table S3. Population density of 12 selected regions in northern slope of Tianshan mountain in 1990, 2000, 2010 and 2020 (104 person/km<sup>2</sup>).

**Author Contributions:** A.K.; methodology, G.A.; software, G.A.; validation, G.A. and A.K.; formal analysis, G.A.; investigation, G.A.; resources, A.K.; data curation, G.A.; writing—original draft preparation, G.A.; writing—review and editing, G.A. and A.K.; visualization, G.A.; supervision, A.K.; project administration, A.K.; funding acquisition, A.K. All authors have read and agreed to the published version of the manuscript.

**Funding:** This study was supported by The Autonomous Region Social Science Foundation Project, grant number NO. 22BJY020; The Special Project for the Construction of Innovation Environment in the Autonomous Region, grant number NO. 2022D04007.

**Institutional Review Board Statement:** Not applicable.

**Informed Consent Statement:** Not applicable.

**Data Availability Statement:** Data will be made available according to specific request.

**Acknowledgments:** We thank the editorial staff and reviewers for their very constructive comments and suggestions, which have contributed to the improvement of the original manuscript.

**Conflicts of Interest:** The authors declare no conflict of interest.

## References

- Alizamir, M.; Othman Ahmed, K.; Shiri, J.; Fakheri Fard, A.; Kim, S.; Heddami, S.; Kisi, O. A New Insight for Daily Solar Radiation Prediction by Meteorological Data Using an Advanced Artificial Intelligence Algorithm: Deep Extreme Learning Machine Integrated with Variational Mode Decomposition Technique. *Sustainability* **2023**, *15*, 11275. [CrossRef]
- Yao, J.; Yuan, W.; Gao, Z.; Liu, H.; Chen, X.; Ma, Y.; Arntzen, E.; McFarland, D. Impact of shifts in vegetation phenology on the carbon balance of a semiarid sagebrush ecosystem. *Remote Sens.* **2022**, *14*, 5924. [CrossRef]
- Chen, S.; Chen, P.; Ding, L.; Pan, D. Assessments of the above-ocean atmospheric CO<sub>2</sub> detection capability of the GAS instrument onboard the next-generation fengyun-3H satellite. *Remote Sens.* **2022**, *14*, 6032. [CrossRef]
- Neubauer, S.C. Comment on “Extreme Level of CO<sub>2</sub> Accumulation into the atmosphere due to the unequal global carbon emission and sequestration” by M. F. Hossain. *Water Air Soil Pollut.* **2022**, *233*, 371. [CrossRef]
- Chien, F.; Hsu, C.-C.; Ozturk, I.; Sharif, A.; Sadiq, M. The role of renewable energy and urbanization towards greenhouse gas emission in top Asian countries: Evidence from advance panel estimations. *Renew. Energy* **2022**, *186*, 207–216. [CrossRef]
- Doś, A.; Błach, J.; Lipowicz, M.; Pattarin, F.; Flori, E. Institutional Drivers of Voluntary Carbon Reduction Target Setting—Evidence from Poland and Hungary. *Sustainability* **2023**, *15*, 11155. [CrossRef]
- Roper, E.; Wang, Y.; Zhang, Z. Numerical investigation of the application of miller cycle and low-carbon fuels to increase diesel engine efficiency and reduce emissions. *Energies* **2022**, *15*, 1783. [CrossRef]
- Paustian, K.; Ravindranath, N.H.; Amstel, A.V. 2006 IPCC Guidelines for National Greenhouse Gas Inventories; International Panel on Climate Change: Geneva, Switzerland, 2006.
- Zhang, C.-Y.; Zhao, L.; Zhang, H.; Chen, M.-N.; Fang, R.-Y.; Yao, Y.; Zhang, Q.-P.; Wang, Q. Spatial-temporal characteristics of carbon emissions from land use change in Yellow River Delta region, China. *Ecol. Indic.* **2022**, *136*, 108623. [CrossRef]
- Svoboda, J.; Štych, P.; Laštovička, J.; Paluba, D.; Kobliuk, N. Random-forest classification of land use, land-use change and forestry (LULUCF) using sentinel-2 data—A case study of Czechia. *Remote Sens.* **2022**, *14*, 1189. [CrossRef]
- Wang, Y.; Wang, M.; Teng, F.; Ji, Y. Remote Sensing Monitoring and Analysis of Spatiotemporal Changes in China’s Anthropogenic Carbon Emissions Based on XCO<sub>2</sub> Data. *Remote Sens.* **2023**, *15*, 3207. [CrossRef]
- Zhao, R.Q.; Huang, X.J.; Xiao, W.C. Misunderstandings and Future Trends of Researches on Land Use Carbon Emissions in China. *China Land Sci.* **2016**, *30*, 83–92.
- Stryczewska, H.D.; Stępień, M.A.; Boiko, O. Plasma and Superconductivity for the Sustainable Development of Energy and the Environment. *Energies* **2022**, *15*, 4092. [CrossRef]
- Wang, Z.; Li, S.; Li, Z. A novel strategy to reduce carbon emissions of heavy oil thermal recovery: Condensation heat transfer performance of flue gas-assisted steam flooding. *Appl. Therm. Eng. Des. Process. Equip. Econ.* **2022**, *205*, 118076–118089. [CrossRef]
- Zhang, Z.; Wan, L.; Dong, C.; Xie, Y.; Yang, C.; Yang, J.; Li, Y. Impacts of Climate Change and Human Activities on the Surface Runoff in the Wuhua River Basin. *Sustainability* **2018**, *10*, 3405. [CrossRef]
- Chen, L.; Hang, Y.; Li, Q. Spatial-Temporal Characteristics and Influencing Factors of Carbon Emissions from Land Use and Land Cover in Black Soil Region of Northeast China Based on LMDI Simulation. *Sustainability* **2023**, *15*, 9334. [CrossRef]

17. Mmonen, A.; Kopsakangas, S.M. Capturing consumers' awareness and the intention to support carbon neutrality through energy efficient consumption. *Energies* **2022**, *15*, 4022. [[CrossRef](#)]
18. Zhang, M.; Tan, J.; Huang, X.; Lai, L.; Chuai, X. A GIS-based approach for estimating land use related carbon emissions—A case study in Henan Province. In Proceedings of the 2013 21st International Conference on Geoinformatics, Kaifeng, China, 20–22 June 2013.
19. Guo, F.; Zhang, Y.; Chang, C.; Yu, Y. Carbon emissions of assembly buildings constrained by flexible resource: A study on cost optimization. *Buildings* **2023**, *13*, 90. [[CrossRef](#)]
20. Liu, M.; Chen, Y.; Chen, K.; Chen, Y. Progress and Hotspots of Research on Land-Use Carbon Emissions: A Global Perspective. *Sustainability* **2023**, *15*, 7245. [[CrossRef](#)]
21. Cui, Y.; Li, L.; Chen, L.; Zhang, Y.; Cheng, L.; Zhou, X.; Yang, X. Land-use carbon emissions estimation for the yangtze river delta urban agglomeration using 1994–2016 landsat image data. *Remote Sens.* **2018**, *10*, 1334. [[CrossRef](#)]
22. Xia, C.; Li, Y.; Xu, T.; Chen, Q.; Ye, Y.; Shi, Z.; Liu, J.; Ding, Q.; Li, X. Analyzing spatial patterns of urban carbon metabolism and its response to change of urban size: A case of the Yangtze River Delta, China. *Ecol. Indic.* **2019**, *104*, 615–625. [[CrossRef](#)]
23. Liu, H.; Yan, F.; Tian, H. Towards low-carbon cities: Patch-based multi-objective optimization of land use allocation using an improved non-dominated sorting genetic algorithm-II. *Ecol. Indic.* **2022**, *134*, 108455. [[CrossRef](#)]
24. Guo, X.; Wang, X.; Wu, X.; Chen, X.; Li, Y. Carbon emission efficiency and low-carbon optimization in Shanxi province under "Dual Carbon" Background. *Energies* **2022**, *15*, 2369. [[CrossRef](#)]
25. Izhar, T.; Xuan, L.P. The estimation of greenhouse gas emission in leachate treatment plant and its carbon credit revenue. *IOP Conf. Ser. Earth Environ. Sci.* **2021**, *646*, 012067. [[CrossRef](#)]
26. Chanu, T.N.; Nag, S.K.; Koushlesh, S.K.; Devi, M.S.; Das, B.K. Greenhouse gas emission from inland open water bodies and their estimation process—An emerging issue in the era of climate change. *Agric. Sci.* **2022**, *13*, 290–306. [[CrossRef](#)]
27. Wang, Q.; Huang, J.; Zhou, H.; Sun, J.; Yao, M. Carbon emission inversion model from provincial to municipal scale based on nighttime light remote sensing and improved STIRPAT. *Sustainability* **2022**, *14*, 6813. [[CrossRef](#)]
28. Yang, X.; Shang, G.; Deng, X. Estimation, decomposition and reduction potential calculation of carbon emissions from urban construction land: Evidence from 30 provinces in China during 2000–2018. *Environ. Dev. Sustain.* **2021**, *24*, 7958–7975. [[CrossRef](#)]
29. Zhang, M.; Lai, L.; Huang, X.J.; Chuai, X.W.; Tan, J.Z. The carbon emission intensity of land use conversion in different regions of China. *Resour. Sci.* **2013**, *35*, 792–799.
30. Ali, G.; Nitivattananon, V. Exercising multidisciplinary approach to assess interrelationship between energy use, carbon emission and land use change in a metropolitan city of Pakistan. *Renew. Sustain. Energy Rev.* **2012**, *16*, 775–786. [[CrossRef](#)]
31. Zhang, L.; Wang, P. Analysis on the change characteristics of the correlation between land use structure and energy consumption and carbon emissions in Kunming from 1997 to 2017. *J. Geosci. Environ. Prot.* **2021**, *9*, 155–166. [[CrossRef](#)]
32. Cai, C.; Fan, M.; Yao, J.; Zhou, L.; Wang, Y.; Liang, X.; Liu, Z.; Chen, S. Spatial-temporal characteristics of carbon emissions corrected by socio-economic driving factors under land use changes in Sichuan Province, southwestern China. *Ecol. Inform.* **2023**, *77*, 102164. [[CrossRef](#)]
33. Derindag, O.F.; Maydybura, A.; Kalra, A.; Wong, W.K.; Chang, B.H. Carbon emissions and the rising effect of trade openness and foreign direct investment: Evidence from a threshold regression model. *Heliyon* **2023**, *9*, e17448. [[CrossRef](#)]
34. Chen, C.; Luo, Y.; Zou, H.; Huang, J. Understanding the driving factors and finding the pathway to mitigating carbon emissions in China's Yangtze River Delta region. *Energy* **2023**, *278*, 127897. [[CrossRef](#)]
35. Wo, R.; Fang, D.; Song, D.; Chen, B. Analysis of embodied carbon emissions and carbon sequestration in Tibetan Plateau-Case study of Tibet and Qinghai. *Appl. Energy* **2023**, *347*, 121449. [[CrossRef](#)]
36. Hung, L.Q.; Asaeda, T.; Thao, V.T.P. Carbon emissions in the field of land use, land use change, and forestry in the Vietnam mainland. *Wetl. Ecol. Manag.* **2021**, *29*, 315–329. [[CrossRef](#)]
37. Gao, P.; Yue, S.J.; Chen, H.T. Carbon emission efficiency of China's industry sectors: From the perspective of embodied carbon emissions. *J. Clean. Prod.* **2020**, *283*, 124655. [[CrossRef](#)]
38. Wang, K.L.; Xu, R.Y.; Jiang, W.; Liu, Y. Impact of National Industrial Relocation Demonstration Zones (NIRDZs) policy on urban carbon emissions in China. *Environ. Impact Assess. Rev.* **2023**, *102*, 107165. [[CrossRef](#)]
39. Wang, Q.; Yang, C.H.; Wang, M.L.; Zhao, L.; Zhao, Y.C.; Zhang, Q.P.; Zhang, C.Y. Decoupling analysis to assess the impact of land use patterns on carbon emissions: A case study in the Yellow River Delta efficient eco-economic zone, China. *J. Clean. Prod.* **2023**, *412*, 137415. [[CrossRef](#)]
40. Xiao, P.; Xu, J.; Yu, Z.; Qian, P.; Lu, M.; Ma, C. Spatiotemporal pattern differentiation and influencing factors of cultivated land use efficiency in hubei province under carbon emission constraints. *Sustainability* **2022**, *14*, 7042. [[CrossRef](#)]
41. Yang, Z.; Zhang, S.; Lei, J.; Zhang, X.; Tong, Y.; Duan, Z.; Fan, L. Evolution of economic linkage network of the cities and counties on the northern slope of the Tianshan Mountains, China. *Reg. Sustain.* **2023**, *4*, 173–184. [[CrossRef](#)]
42. Yu, T.; Abulizi, A.; Xu, Z.; Jiang, J.; Akbar, A.; Ou, B.; Xu, F. Evolution of environmental quality and its response to human disturbances of the urban agglomeration in the northern slope of the Tianshan Mountains. *Ecol. Indic.* **2023**, *153*, 110481. [[CrossRef](#)]
43. Wang, S.; Tan, S.; Xu, J. Evaluation and Implication of the Policies towards China's Carbon Neutrality. *Sustainability* **2023**, *15*, 6762. [[CrossRef](#)]

44. Zhao, M.; Cheng, W.M.; Huang, K.; Wang, N.; Liu, Q. Research on land cover change in Beijing-Tianjin-Hebei region during the last 10 years based on different geomorphic units. *J. Nat. Resour.* **2016**, *31*, 252–264.
45. Chen, X.; Luo, G.; Xia, J.; Zhou, K.; Lou, S.; Ye, M. Ecological response to the climate change on the northern slope of the Tianshan Mountains in Xinjiang. *Sci. China Ser. D Earth Sci.* **2005**, *48*, 765–777. [[CrossRef](#)]
46. Zhi, X.; Anfuding, G.; Yang, G.; Gong, P.; Wang, C.; Li, Y.; Li, X.; Li, P.; Liu, C.; Qiao, C.; et al. Evaluation of the water resource carrying capacity on the North Slope of the Tianshan Mountains, Northwest China. *Sustainability* **2022**, *14*, 1905. [[CrossRef](#)]
47. Ma, H.; Sun, J. The influence of LUCC on water demand in the north slope of Tianshan Mountain. *IOP Conf. Ser. Earth Environ. Sci.* **2020**, *560*, 012079. [[CrossRef](#)]
48. Li, B.; Chong, J.; Liu, H.; Hong, R.; Zhang, S.-H.; Zhang, X.-S. Study on the spatio-temporal changes of ecosystem service value in the northern slope of Tianshan Mountains. *Int. Geosci. Remote Sens. Symp.* **2009**, *2*, 335–338.
49. Duan, F.; An, C.; Wang, W.; Herzschuh, U.; Zhang, M.; Zhang, H.; Liu, Y.; Zhao, Y.; Li, G. Dating of a late Quaternary loess section from the northern slope of the Tianshan Mountains (Xinjiang, China) and its paleoenvironmental significance. *Quat. Int.* **2020**, *544*, 104–112. [[CrossRef](#)]
50. Zhuang, Q.; Shao, Z.; Li, D.; Huang, X.; Cai, B.; Altan, O.; Wu, S. Unequal weakening of urbanization and soil salinization on vegetation production capacity. *Geoderma* **2022**, *411*, 115712–115720. [[CrossRef](#)]
51. Song, Y.; Luo, D.; Du, J.; Kang, S.; Cheng, P.; Fu, C.; Guo, X. Radiometric dating of late Quaternary loess in the northern piedmont of South Tianshan Mountains: Implications for reliable dating. *Geol. J.* **2018**, *53*, 417–426. [[CrossRef](#)]
52. Fan, Z.H. Analysis on the coupling degree of water source ecological environment based on 3S technology. *Int. J. Environ. Technol. Manag.* **2022**, *25*, 324–336. [[CrossRef](#)]
53. Luo, G.; Feng, Y.; Zhang, B.; Cheng, W. Sustainable land-use patterns for arid lands: A case study in the northern slope areas of the Tianshan Mountains. *J. Geogr. Sci.* **2010**, *20*, 510–524. [[CrossRef](#)]
54. Qing, Y.; Zhao, B.; Wen, C. The coupling and coordination of agricultural carbon emissions efficiency and economic growth in the Yellow River Basin, China. *Sustainability* **2023**, *15*, 971. [[CrossRef](#)]
55. Chen, H.; Wang, B.; Wang, W.; Wang, S. Using nighttime light data to achieve precise estimation of residents' living carbon emissions and landscape pattern characteristics. In Proceedings of the 2022 International Conference on Green Building, Civil Engineering and Smart City, Guilin, China, 8–10 April 2022; pp. 65–77.
56. Houghton, R.A.; Van der Werf, G.R.; DeFries, R.S.; Hansen, M.C.; House, J.I.; Le Quéré, C.; Pongratz, J.; Ramankutty, N. Carbon emissions from land use and land-cover change. *Biogeosci. Discuss.* **2012**, *9*, 835–878. [[CrossRef](#)]
57. Bai, X.; Chen, J.; Shi, P. Landscape urbanization and economic growth in China: Positive feedbacks and sustainability dilemmas. *Environ. Sci. Technol.* **2012**, *46*, 132–139. [[CrossRef](#)] [[PubMed](#)]
58. Lai, L.; Huang, X.; Yang, H.; Chuai, X.; Zhang, M.; Zhong, T.; Chen, Z.; Chen, Y.; Wang, X.; Thompson, J.R. Carbon emissions from land-use change and management in China between 1990 and 2010. *Sci. Adv.* **2016**, *2*, e1601063. [[CrossRef](#)]
59. Shi, D.; Lu, X. Accumulation degree and source apportionment of trace metals in smaller than 63  $\mu\text{m}$  road dust from the areas with different land uses: A case study of Xi'an, China. *Sci. Total Environ.* **2018**, *636*, 1211–1218. [[CrossRef](#)]
60. Xia, L.; Zhang, Y.; Sun, X.; Li, J. Analyzing the spatial pattern of carbon metabolism and its response to change of urban form. *Ecol. Model.* **2017**, *355*, 105–115. [[CrossRef](#)]
61. Pessôa, A.C.M.; Anderson, L.O.; Carvalho, N.S.; Campanharo, W.A.; Junior, C.H.L.S.; Rosan, T.M.; Reis, J.B.C.; Pereira, F.R.S.; Assis, M.; Jacon, A.D.; et al. Intercomparison of burned area products and its implication for carbon emission estimations in the Amazon. *Remote Sens.* **2020**, *12*, 3864. [[CrossRef](#)]
62. Diao, J.; Liu, J.; Zhu, Z.; Li, M.; Sleeter, B.M. Substantially greater carbon emissions estimated based on annual land-use transition data. *Remote Sens.* **2020**, *12*, 1126. [[CrossRef](#)]
63. Ray, R.L.; Ibrionke, A.; Kommalapati, R.; Fares, A. Quantifying the impacts of land-use and climate on carbon fluxes using satel-lite data across Texas, U.S. *Remote Sens.* **2019**, *11*, 1733. [[CrossRef](#)]
64. Fu, W.J.; Jiang, P.K.; Zhou, G.M.; Zhao, K.L. Using Moran's I and GIS to study the spatial pattern of forest litter carbon density in a subtropical region of southeastern China. *Biogeosciences* **2014**, *11*, 2401–2414. [[CrossRef](#)]
65. Keshavarzi, A.; Bhunia, G.S.; Shit, P.K.; Ertunç, G.; Zeraatpisheh, M. Spatial pattern analysis and identifying soil pollution hotspots using local Moran's I and GIS at a regional scale in northeast of Iran. In *Soil Health and Environmental Sustainability: Application of Geospatial Technology*; Springer International Publishing: Cham, Switzerland, 2022; pp. 283–307.
66. Rong, T.; Zhang, P.; Jing, W.; Zhang, Y.; Li, Y.; Yang, D.; Yang, J.; Chang, H.; Ge, L. Carbon dioxide emissions and their driving forces of land use change based on economic contributive coefficient (ECC) and ecological support coefficient (ESC) in the lower Yellow River Region (1995–2018). *Energies* **2020**, *13*, 2600. [[CrossRef](#)]
67. Duc, H.N.; Azzi, M.; Zhang, Y.; Kirkwood, J.; White, S.; Trieu, T.; Riley, M.; Salter, D.; Chang, L.T.-C.; Capnerhurst, J.; et al. Black Carbon Emissions, Transport and Effect on Radiation Forcing Modelling during the Summer 2019–2020 Wildfires in Southeast Australia. *Atmosphere* **2023**, *14*, 699. [[CrossRef](#)]
68. Ghosh, S.; Dinda, S.; Chatterjee, N.D.; Dutta, S.; Bera, D. Spatial-explicit carbon emission-sequestration balance estimation and evaluation of emission susceptible zones in an Eastern Himalayan city using Pressure-Sensitivity-Resilience framework: An approach towards achieving low carbon cities. *J. Clean. Prod.* **2022**, *336*, 130417–130429. [[CrossRef](#)]

69. Zhang, J.; Li, S.; Lin, N.; Lin, Y.; Yuan, S.; Zhang, L.; Zhu, J.; Wang, K.; Gan, M.; Zhu, C. Spatial identification and trade-off analysis of land use functions improve spatial zoning management in rapid urbanized areas, China. *Land Use Policy* **2022**, *116*, 106058–106072. [[CrossRef](#)]
70. Ran, L.; Wang, X.; Li, S.; Zhou, Y.; Xu, Y.; Chan, C.N.; Fang, N.; Xin, Z.; Shen, H. Integrating aquatic and terrestrial carbon fluxes to assess the net landscape carbon balance of a highly erodible semiarid catchment. *J. Geophys. Res. Biogeosci.* **2022**, *127*, 6765–6780. [[CrossRef](#)]
71. Zhao, R.Q.; Zhang, S.; Huang, X.J.; Qin, Y.C.; Liu, Y.; Ding, M.; Jiao, S. Spatial variation of carbon budget and carbon balance zoning of Central Plains Eco-nomic Region at county-level. *Acta Geogr. Sin.* **2014**, *69*, 1425–1437.
72. Wei, B.; Kasimu, A.; Rehemani, R.; Zhang, X.; Zhao, Y.; Aizizi, Y.; Liang, H. Spatiotemporal characteristics and prediction of carbon emissions/absorption from land use change in the urban agglomeration on the northern slope of the Tianshan Mountains. *Ecol. Indic.* **2023**, *151*, 110329. [[CrossRef](#)]

**Disclaimer/Publisher’s Note:** The statements, opinions and data contained in all publications are solely those of the individual author(s) and contributor(s) and not of MDPI and/or the editor(s). MDPI and/or the editor(s) disclaim responsibility for any injury to people or property resulting from any ideas, methods, instructions or products referred to in the content.